Explicit Magnus expansions for solving the time-dependent Schrödinger equation

2008 J. Phys. A: Math. Theor. 41 295203

(http://iopscience.iop.org/1751-8121/41/29/295203)

IOP PUBLISHING JOURNAL OF PHYSICS A: MATHEMATICAL AND THEORETICAL

J. Phys. A: Math. Theor. **41** (2008) 295203 (25pp) doi:10.1088/1751-8113/41/29/295203

Explicit Magnus expansions for solving the time-dependent Schrödinger equation

O Chuluunbaatar[1], V L Derbov[2], A Galtbayar[3], A A Gusev[1], M S Kaschiev[4,5], S I Vinitsky[1] and T Zhanlav[3]

[1] Joint Institute for Nuclear Research, Dubna, Moscow Region 141980, Russia
[2] Saratov State University, Saratov, 410012, Russia
[3] National University of Mongolia, Ulaanbaatar, Mongolia
[4] Institute of Mathematics and Informatics, BAS, Sofia, Bulgaria

Received 27 February 2008, in final form 30 May 2008
Published 26 June 2008
Online at stacks.iop.org/JPhysA/41/295203

Abstract

The symmetric implicit operator-difference multi-layer schemes for solving the time-dependent Schrödinger equation based on decomposition of the evolution operator via the explicit Magnus expansion up to the sixth order of accuracy with respect to the time step are presented. Reduced schemes for solving the set of coupled time-dependent Schrödinger equations with respect to the hyper-radial variable are devised by using the Kantorovich expansion of the wave packet over a set of appropriate parametric basis angular functions. Further discretization of the resulting problem with symmetric operators is implemented by means of the finite-element method. The convergence and efficiency of the numerical schemes are demonstrated in benchmark calculations of the exactly solvable models of a one-dimensional time-dependent oscillator, a two-dimensional oscillator in time-dependent electric field by using the conventual angular basis, and the inexactly solvable model of a three-dimensional kicked hydrogen atom in a magnetic field by using a parametric basis of the angular oblate spheroidal functions developed in our previous paper (Chuluunbaatar O *et al* 2007 *J. Phys. A: Math. Theor.* **40** 11485–524).

PACS numbers: 02.30.Jr, 02.60.Lj, 02.70.Dh, 03.65.−w, 31.15.Ja, 31.15.Pf

1. Introduction

Modern laser physics experiments have stimulated computer simulations [1–3] related to the time-dependent dynamics of few-body Coulomb systems in a train of laser pulses [4–6] and the time-dependent Schrödinger equation (TSDE) involved in the control problems of finite-

[5] It is painful to think Professor M S Kaschiev is no longer among us, and this paper is his last contribution to TDSE solving on the base of the finite-element method which owes remarkable results to him. His intuition, insight and support were invaluable for other authors during our long-standing collaboration. We are deeply grateful to him.

dimensional quantum systems [7] and magnetic traps [8–12]. For any numerical method two requirements are of principal importance: one is stability, and the other is accuracy. From the viewpoint of these requirements, the unitary splitting methods have a big advantage: the unitarity of the evolution operators applied preserves the norm of the wavefunctions, so that the conservation of probability density and the robustness of the numerical schemes are guaranteed.

Solving the TDSE with prescribed accuracy is necessary for control problems in finite-dimensional quantum systems [7], decay problem in nuclear physics [13], de-excitation of antihydrogen atoms [12], ionization problems in atoms and molecules excited by pulsed fields [6] or impact collisions beyond the dipole approximation [14, 15]. For solving the TDSE in a finite spatial region [16, 17] one usually seeks for a wave-packet solution in the form of expansion over the appropriate angular basis functions, and then performs proper discretization of hyper-radial equations, e.g., using the finite-difference [14, 18, 19], finite-element [5, 20], spline [16, 21] methods, etc.

In the present paper a new computational method is proposed to solve the TDSE, in which the unitary explicit splitting algorithms for decomposition of the evolution operator via the Magnus expansion [22] on uniform time grids [3, 23–25] is combined with the Kantorovich or Galerkin reduction to a set of hyper-radial TDSEs [20], the finite-element method (FEM) [26, 27] and the interpolation on nonuniform spatial grids [20, 28, 29]. The efficiency and accuracy of the developed reductions and numerical schemes are demonstrated for several integrable atomic models in external fields.

Usually the rate convergence with respect to the number of angular basis functions is controlled by solving the corresponding stationary Schrödinger equation [30]. However, some special cases of long-range effective potentials acting in asymptotic regions, such as confinement potentials, require additional analysis [18], which is the key problem. Numerical solution of TDSEs describing exactly solvable models can provide useful information for such analysis.

The organization of this paper is outlined as follows. In section 2, the general formulation and the operator-difference multi-layer (ODML) calculation scheme for solving the time-dependent operator differential equation in a finite time interval are given. In section 3, the application of the considered scheme for the TDSE with the Kantorovich approach up to the sixth order with respect to the time step is presented. The basic structure of the numerical calculation for the generation of the matrix problem in the framework of FEM is described in section 4. In section 5, the stability and efficiency of the developed schemes and algorithms are confirmed in exactly solvable models, namely, a one-dimensional time-dependent oscillator and a two-dimensional oscillator in a time-dependent electric field, as well as an inexactly solvable model, namely, a three-dimensional kicked hydrogen atom in a magnetic field. Section 6 is devoted to concluding remarks and perspectives of further studies.

2. General formulation and ODML calculation scheme

Consider the Cauchy problem for the time-dependent operator equation in the time interval $t \in [t_0, T]$

$$\mathrm{i}\frac{\partial \Psi(t)}{\partial t} = H(t)\Psi(t), \qquad \Psi(t_0) = \Psi_0, \tag{1}$$

where $H(t)$ is a linear self-adjoint operator. We rewrite equation (1) in terms of a unitary evolution operator $U(t, t_0, \lambda)$ with the complementary formal parameter λ [6] transforming the

[6] The complementary formal parameter λ will be later given a definite value $\lambda = 1$.

initial state Ψ_0 into the solution $\Psi(t)$

$$\mathrm{i}\frac{\partial U(t,t_0,\lambda)}{\partial t} = \lambda H(t)U(t,t_0,\lambda), \qquad U(t,t,\lambda) = 1. \tag{2}$$

Introduce a uniform grid $\Omega_\tau[t_0,T] = \{t_0, t_{k+1} = t_k + \tau, t_K = T\}$ with the time step τ, covering the time interval $[t_0,T]$. For each step we express the unitary operator $U(t_{k+1},t_k,\lambda)$ transforming $\Psi(t_k)$ at $t = t_k (k = 0,\ldots,K-1)$ into $\Psi(t_{k+1})$ at $t = t_{k+1}$ in the form [23, 24]

$$\begin{aligned} &\Psi(t_{k+1}) = U(t_{k+1},t_k,\lambda)\Psi(t_k), \\ &U(t_{k+1},t_k,\lambda) = \exp\left(-\mathrm{i}\tau A_k^{(M)}(t_{k+1},\lambda)\right) + O(\tau^{2M+1}). \end{aligned} \tag{3}$$

2.1. Implicit decomposition of the evolution operator

We start with the expansion of $A_k^{(M)}(t) \equiv A_k^{(M)}(t,\lambda)$ in powers of the formal parameter λ,

$$A_k^{(M)}(t,\lambda) = \frac{\mathrm{i}}{\tau}\sum_{j=1}^{2M}\lambda^j A_{(j)k}(t), \qquad A_k^{(M)}(t_k,\lambda) = 0, \tag{4}$$

where the coefficients $A_{(j)}(t) \equiv A_{(j)k}(t)$ are determined by the operator identity [31]

$$-\mathrm{i}\lambda H(t) = \sum_{n=1;q=0;l_1,\ldots,l_q=1}^{n+\Sigma_{i=1}^q l_i \leqslant 2M} \frac{\lambda^{n+\Sigma_{i=1}^q l_i}}{(q+1)!}(adA_{(l_1)}(t))\ldots(adA_{(l_q)}(t))\dot{A}_{(n)}(t). \tag{5}$$

Here the linear operator $(adA) : \mathcal{L}(X) \to \mathcal{L}(X)$ ($\mathcal{L}(X)$ is the space of linear operators) is defined for operators $A, B \in \mathcal{L}(X)$ in the form $(adA)B = [A,B] \equiv AB - BA$, and has the following properties: $(adA)^0 B = B$, $(adA)^j B = (adA)^{j-1}(adA)B$. Note that the dot over the operator $A_{(n)}(t)$ means the partial derivative, $\dot{A}_{(n)}(t) = \partial_t A_{(n)}(t)$, in t. Equating the coefficients at the same powers of λ on both sides of equation (5), we obtain a set of first-order differential equations [2]. For example, the first three equations are

$$\begin{aligned} &\dot{A}_{(1)}(t) = -\mathrm{i}H(t), \\ &\dot{A}_{(2)}(t) = -\tfrac{1}{2}(adA_{(1)}(t))\dot{A}_{(1)}(t), \\ &\dot{A}_{(3)}(t) = -\tfrac{1}{2}(adA_{(2)}(t))\dot{A}_{(1)}(t) - \tfrac{1}{6}(adA_{(1)}(t))^2\dot{A}_{(1)}(t) - \tfrac{1}{2}(adA_{(1)}(t))\dot{A}_{(2)}(t). \end{aligned} \tag{6}$$

Therefore, we obtain

$$A_{(1)}(t) = -\mathrm{i}\Upsilon_1^1(t), \qquad A_{(2)}(t) = \frac{1}{2}\Upsilon_{21}^2(t), \qquad A_{(3)}(t) = \frac{\mathrm{i}}{6}\left(\Upsilon_{123}^3(t) + \Upsilon_{321}^3(t)\right). \tag{7}$$

The fourth-order term is calculated in the same way. We find

$$A_{(4)}(t) = \tfrac{1}{12}\left(\Upsilon_{1432}^4(t) + \Upsilon_{1234}^4(t) + \Upsilon_{4312}^4(t) + \Upsilon_{2341}^4(t)\right). \tag{8}$$

Here

$$\Upsilon_{l_1,\ldots,l_n}^n(t) = \int_{t_k}^{t} \mathrm{d}t_1 \int_{t_k}^{t_1} \mathrm{d}t_2 \ldots \int_{t_k}^{t_{n-1}} \mathrm{d}t_n (adH(t_{l_1}))\ldots(adH(t_{l_{n-1}}))H(t_{l_n}). \tag{9}$$

Note that the fourth-order formula (8) agrees with [31, 32], but does not agree with [33, 34] because of misprints in these papers.

Solving sequentially the set of equations thus obtained, we arrive at effective Hamiltonians $A_k^{(M)}(t)$ connected with the original one $H(t)$ via the Magnus expansion [22] written in terms of repeated integrals [31]. We would like to express the truncation $A_k^{(M)}(t)$ in terms of $H(t)$ and its time partial derivatives. Substituting the Taylor expansion of $H(t)$ in the vicinity of $t_c = t_k + \tau/2$,

$$H(t) = \sum_{j=0}^{2M-1} \frac{(t-t_c)^j}{j!} \partial_t^j H(t_c) + O(\tau^{2M}), \tag{10}$$

into the integrals, one can derive an analytical expression of the operators $A_k^{(1)}(t)$, $A_k^{(2)}(t)$, $\ldots$, $A_k^{(M)}(t)$ by means of the symbolic algorithm GATEO (generation of approximations of the time-evolution operator) [2]. Indeed, for $A_k^{(1)}(t)$ one should only calculate the coefficient of λ^1, and then obtain

$$A_k^{(1)}(t_{k+1}) = \int_0^1 \mathrm{d}\xi\, H(t_k + \xi\tau) = H(t_c) + O(\tau^2), \tag{11}$$

without any difficulties. However, in the case of $A_k^{(M)}(t)$ with large M, rather cumbersome calculations are required to find all the coefficients 'by hand'.

2.2. Explicit decomposition of the evolution operator

For the expansion of the Hamiltonian $H(t)$ in the vicinity of $t = t_c$ we can also find the operators $A_k^{(M)}(t_{k+1})$ in the form of a series at $\lambda = 1$,

$$A_k^{(M)}(t_{k+1}) = \sum_{j=0}^{2M-1} \tau^j \check{A}_{(j)}(t_c), \tag{12}$$

with unknown coefficients $\check{A}_{(j)}(t_c)$. Recalling that the evolution operator $U(t_k, t_{k+1}, \lambda)$ is inverse to the operator $U(t_{k+1}, t_k, \lambda)$, we get $A_{k+1}^{(M)}(t_k) = A_k^{(M)}(t_{k+1})$. It means that the series of $A_k^{(M)}(t_{k+1})$ written above contains only even powers of τ because the expression of $A_{k+1}^{(M)}(t_k)$ is obtained from $A_k^{(M)}(t_{k+1})$ by a formal substitution $\tau \to -\tau$. Then the unknown coefficients $\check{A}_{(j)}(t_c)$ are calculated explicitly from a set of recurrence equations (see the appendix A)

$$\begin{aligned}
&(j+1)\check{A}_{(j)}(t_c) = \frac{1+(-1)^j}{2^{j+1} j!} \partial_t^j H(t_c) + \sum_{q=1}^{j} \sum_{n=0}^{j-q} \sum_{l_1,\ldots,l_q=0}^{n+q+\sum_{i=1}^q l_i = j} \frac{(-\mathrm{i})^q B^n_{l_1,\ldots,l_q}(t_c)}{q!}, \\
&B^n_{l_1,\ldots,l_q}(t_c) = (ad\check{A}_{(l_1)}(t_c)) \ldots (ad\check{A}_{(l_q)}(t_c)) Q_{qn}(t_c), \\
&Q_{qn}(t_c) = \frac{(-1)^n}{2^{n+1} n!} \partial_t^n H(t_c) - \frac{n+1}{q+1} \check{A}_{(n)}(t_c).
\end{aligned} \tag{13}$$

To show the complexity of calculations, we present the first three approximations of the exponential (3) for the final effective Hamiltonians $A_k^{(M)} \equiv A_k^{(M)}(t_{k+1})$ in the form $A_k^{(M)} = \hat{A}_k^{(M)} + \mathrm{i}\check{A}_k^{(M)}$,

$$\begin{aligned}
\hat{A}_k^{(1)} &= H, \\
\check{A}_k^{(1)} &= 0, \\
\hat{A}_k^{(2)} &= \hat{A}_k^{(1)} + \frac{\tau^2}{24} \ddot{H}, \\
\check{A}_k^{(2)} &= \check{A}_k^{(1)} + \frac{\tau^2}{12} (adH)\dot{H},
\end{aligned}$$

Table 1. Real and imaginary parts of the coefficients $\alpha_\zeta^{(M)}$, $M = 1, 2, 3$, $\zeta = 1, \ldots, M$.

M	ζ	$\Re\alpha_\zeta^{(M)}$	$\Im\alpha_\zeta^{(M)}$
1	1	+0.0	−1.0
2	1	−0.577 350 269 189 625 764 509 148 780 50	−1.0
2	2	+0.577 350 269 189 625 764 509 148 780 50	−1.0
3	1	−0.814 799 554 248 922 818 414 736 231 56	−0.854 056 730 651 663 465 265 799 408 86
3	2	+0.0	−1.291 886 538 696 673 069 468 401 182 28
3	3	+0.814 799 554 248 922 818 414 736 231 56	−0.854 056 730 651 663 465 265 799 408 86

$$\hat{A}_k^{(3)} = \hat{A}_k^{(2)} + \frac{\tau^4}{1920}\dddot{\dddot{H}} - \frac{\tau^4}{720}(ad\,H)^2\ddot{H} - \frac{\tau^4}{240}(ad\,\dot{H})^2 H,$$
$$\check{A}_k^{(3)} = \check{A}_k^{(2)} - \frac{\tau^4}{480}(ad\,\dddot{H})H + \frac{\tau^4}{480}(ad\,\ddot{H})\dot{H} + \frac{\tau^4}{720}(ad\,H)^3\dot{H}, \tag{14}$$

where $H \equiv H(t_c)$, $\dot{H} \equiv \partial_t H(t)|_{t=t_c}, \ldots$

2.3. Implicit ODML schemes

We wish to make further approximation of the unitary scheme [23, 24] of equation (3). The application of the generalized $[M/M]$ Padé approximation to the exponential operator yields

$$\exp\left(-\mathrm{i}\tau A_k^{(M)}\right) = \prod_{\zeta=M}^{1} T_{\zeta k} + O(\tau^{2M+1}),$$
$$T_{\zeta k} = \left(I + \frac{\tau\overline{\alpha}_\zeta^{(M)} A_k^{(M)}}{2M}\right)^{-1}\left(I + \frac{\tau\alpha_\zeta^{(M)} A_k^{(M)}}{2M}\right), \tag{15}$$

where I is the unit operator and the overline indicates the complex conjugate. The coefficients, $\alpha_\zeta^{(M)}$ ($\zeta = 1, \ldots, M$, $M \geqslant 1$), stand for the roots of the polynomial equation, ${}_1F_1(-M, -2M, 2M\mathrm{i}/\alpha) = 0$, where ${}_1F_1$ is the confluent hypergeometric function. The properties of the zeros of this polynomial have been well studied [35–37]. Table 1 lists the values of the coefficients, $\alpha_\zeta^{(M)}$ for $M = 1, 2, 3$, in GATEO. The coefficients $\alpha_\zeta^{(M)}$ have the following properties: $\Im\,\alpha_\zeta^{(M)} < 0$ and $0.6 < \left|\alpha_\zeta^{(M)}\right| < \mu^{-1}$, where $\mu \approx 0.28$ is the root of the equation $\mu\exp(\mu + 1) = 1$ [23]. Note that the condition

$$\tau < 2M\mu\left\|A_k^{(M)}(t)\right\|^{-1}, \tag{16}$$

guarantees the validity of the approximation (15) for any bounded operator $A_k^{(M)}(t)$.

We are now in a position to obtain the transition from $\Psi(t_k)$ to $\Psi(t_{k+1})$ using the approximation (15) of the evolution operator in (3). For this purpose we rewrite the transition in terms of the auxiliary functions defined by

$$\psi_k^0 = \Psi(t_k),$$
$$\left(I + \frac{\tau\overline{\alpha}_\zeta^{(M)} A_k^{(M)}}{2M}\right)\psi_k^{\zeta/M} = \left(I + \frac{\tau\alpha_\zeta^{(M)} A_k^{(M)}}{2M}\right)\psi_k^{(\zeta-1)/M}, \qquad \zeta = 1, \ldots, M, \tag{17}$$
$$\Psi(t_{k+1}) = \psi_k^1.$$

Note that this approach preserves the unitarity of the approximate evolution operator, since the truncated $A_k^{(M)}$ is always self-adjoint. $\mathrm{Im}\,\alpha_\zeta^{(M)} \neq 0$ yields the operators $T_{\zeta k}$ to be isometric, so that all the functions $\psi_k^{\zeta/M}$ have an equal norm, $\left\|\psi_k^0\right\| = \left\|\psi_k^{1/M}\right\| = \cdots = \left\|\psi_k^1\right\|$.

2.4. Symmetric implicit ODML schemes

To generate the schemes with extraction of the symmetric part $\tilde{A}_k^{(M)}(t)$ of the operator $A_k^{(M)}(t)$, we apply a gauge transformation $\tilde{\psi} = \exp\left(\mathrm{i}S_k^{(M)}(t)\right)\psi$ that yields a new operator

$$\tilde{A}_k^{(M)}(t) = \exp\left(\mathrm{i}S_k^{(M)}(t)\right)A_k^{(M)}(t)\exp\left(-\mathrm{i}S_k^{(M)}(t)\right), \tag{18}$$

in accordance with the well-known formula

$$\exp(A)B\exp(-A) = \sum_{j=0}\frac{1}{j!}(adA)^j B. \tag{19}$$

We seek for $S_k^{(M)}(t)$ in the form of a power series with respect to τ

$$S_k^{(M)}(t) = \sum_{j=0}^{2M-1}\tau^j S_{(j)}(t), \tag{20}$$

where the unknown coefficients $S_{(j)}(t)$ are found from the additional condition

$$\overset{\succ}{A}{}_k^{(M)} = \exp\left(\mathrm{i}S_k^{(M)}(t_{k+1})\right)\check{A}_k^{(M)}\exp\left(-\mathrm{i}S_k^{(M)}(t_{k+1})\right) = O(\tau^{2M}). \tag{21}$$

Substituting the expansion of $S_k^{(M)} \equiv S_k^{(M)}(t_{k+1})$ into this condition and equating the terms with the same powers of τ, we obtain a set of algebraic (or operator) recurrence relations for evaluating the unknown coefficients $S_{(j)} \equiv S_{(j)}(t_{k+1})$ with the initial condition $S_{(0)} = 0$. The first three approximations of the operators (20) and (18) have the form

$$\begin{aligned} S_k^{(1)} &= 0, \\ S_k^{(2)} &= S_k^{(1)} + \frac{\tau^2}{12}\dot{H}, \\ S_k^{(3)} &= S_k^{(2)} + \frac{\tau^4}{480}\dddot{H} + \frac{\tau^4}{720}(adH)^2\dot{H}, \qquad \text{if} \quad (ad\ddot{H})\dot{H} \equiv 0, \end{aligned} \tag{22}$$

and

$$\begin{aligned} \tilde{A}_k^{(1)} &= \hat{A}_k^{(1)} = H, \\ \tilde{A}_k^{(2)} &= \hat{A}_k^{(2)} = \tilde{A}_k^{(1)} + \frac{\tau^2}{24}\ddot{H}, \\ \tilde{A}_k^{(3)} &= \hat{A}_k^{(3)} + \frac{\tau^4}{288}(ad\dot{H})^2 H = \tilde{A}_k^{(2)} + \frac{\tau^4}{1920}\ddddot{H} - \frac{\tau^4}{720}(adH)^2\ddot{H} - \frac{\tau^4}{1440}(ad\dot{H})^2 H. \end{aligned} \tag{23}$$

Performing the above procedures at each kth time step of the grid $\Omega_\tau[t_0, T]$ ($k = 0, 1, \ldots, K-1$), we arrive at the operator-difference scheme with partial splitting of the evolution operator

$$\begin{aligned} &\tilde{\psi}_k^0 = \exp\left(\mathrm{i}S_k^{(M)}\right)\Psi(t_k), \\ &\left(I + \frac{\tau\overline{\alpha}_\zeta^{(M)}\tilde{A}_k^{(M)}}{2M}\right)\tilde{\psi}_k^{\zeta/M} = \left(I + \frac{\tau\alpha_\zeta^{(M)}\tilde{A}_k^{(M)}}{2M}\right)\tilde{\psi}_k^{(\zeta-1)/M}, \qquad \zeta = 1, \ldots, M, \\ &\Psi(t_{k+1}) = \exp\left(-\mathrm{i}S_k^{(M)}\right)\tilde{\psi}_k^1. \end{aligned} \tag{24}$$

Hence, the auxiliary functions $\tilde{\psi}_k^{\zeta/M}$ in equation (24) can be treated as a kind of approximate solutions on a set of fractional time steps $t_{k+\zeta/M} = t_k + \tau\zeta/M$, $\zeta = 1, \ldots, M-1$ in the time interval $[t_k, t_{k+1}]$. The scheme (24) is an implicit scheme of the order $2M$, preserving the norm of the difference solution, and hence, is stable. Furthermore, the scheme (24) provides an approximation of the order $O(\tau^{2M})$ in the sense of [38], while any individual equation in

(24) provides only an approximation of the order not higher than $O(\tau^2)$. Note that in the case $M = 1$, i.e., [1/1] Padé approximation of exponential operator (15), the scheme (24) appears to be reduced to the well-known Crank–Nicolson scheme [39].

We wish to construct the generalized $[L/L]$ Padé approximation for $\exp\left(\mathrm{i}S_k^{(M)}\right)$ in analogy with (15). This approximation has the order $O(\tau^{4L+2})$, while $4L + 2 \geqslant 2M$, so that we can choose $L = \left[\frac{M}{2}\right]$, where $[x]$ is the integer part of x. In this case we obtain the following modification of the numerical scheme (24):

$$
\begin{aligned}
&\psi_k^0 = \Psi(t_k),\\
&\left(I - \frac{\overline{\alpha}_\eta^{(L)} S_k^{(M)}}{2L}\right)\psi_k^{\eta/L} = \left(I - \frac{\alpha_\eta^{(L)} S_k^{(M)}}{2L}\right)\psi_k^{(\eta-1)/L}, \qquad \eta = 1,\ldots,L,\\
&\tilde{\psi}_k^0 = \psi_k^1,\\
&\left(I + \frac{\tau\overline{\alpha}_\zeta^{(M)} \tilde{A}_k^{(M)}}{2M}\right)\tilde{\psi}_k^{\zeta/M} = \left(I + \frac{\tau\alpha_\zeta^{(M)} \tilde{A}_k^{(M)}}{2M}\right)\tilde{\psi}_k^{(\zeta-1)/M}, \qquad \zeta = 1,\ldots,M,\\
&\psi_k^0 = \tilde{\psi}_k^1,\\
&\left(I + \frac{\overline{\alpha}_\eta^{(L)} S_k^{(M)}}{2L}\right)\psi_k^{\eta/L} = \left(I + \frac{\alpha_\eta^{(L)} S_k^{(M)}}{2L}\right)\psi_k^{(\eta-1)/L}, \qquad \eta = 1,\ldots,L,\\
&\Psi(t_{k+1}) = \psi_k^1.
\end{aligned}
\tag{25}
$$

Theorem. *Let the operator $A_k^{(M)}(t)$ satisfy the bounding condition (16) for the given time step τ, then the error of the numerical schemes (17) and (25) is bounded by*

$$\epsilon_M = \|\Psi_{\mathrm{ext}}(t_{k+1}) - \Psi(t_{k+1})\| \leqslant C\tau^{2M}(t_{k+1} - t_0) \max_{t_0 \leqslant t \leqslant t_{k+1}} \|H^{2M+1}(t)\Psi_{\mathrm{ext}}(t)\|, \tag{26}$$

where $\Psi_{\mathrm{ext}}(t_{k+1})$ is the exact solution of the evolution equation (1) at the time moment $t = t_{k+1}$, $\Psi(t_{k+1})$ is its approximate solution, and C is a constant.

The proof is similar to given in that [40].

3. Application of the scheme to TDSE

Let us consider a d-dimensional TDSE with the Hamiltonian $H(t) \equiv H(\mathbf{r}, t)$

$$\mathrm{i}\frac{\partial\Psi(\mathbf{r}, t)}{\partial t} = H(\mathbf{r}, t)\Psi(\mathbf{r}, t), \qquad \Psi(\mathbf{r}, t_0) = \Psi_0(\mathbf{r}), \tag{27}$$

where the Hamiltonian with a governing function $f(\mathbf{r}, t)$ in the time interval $t \in [t_0, T]$ has the form

$$H(\mathbf{r}, t) = H_0(\mathbf{r}) + f(\mathbf{r}, t), \qquad H_0(\mathbf{r}) = -\tfrac{1}{2}\nabla_{\mathbf{r}}^2 + U(\mathbf{r}). \tag{28}$$

We require the solutions $\Psi(\mathbf{r}, t)$ to be continuous and to have general first derivatives integrable with square, and to belong to the Sobolev space $\mathbf{W}_2^1(\mathbf{R}^d \otimes [t_0, T])$, i.e. $\Psi(\mathbf{r}, t) \in \mathbf{W}_2^1(\mathbf{R}^d \otimes [t_0, T])$. We suppose that these solutions describe an atomic model in the external field $f(\mathbf{r}, t)$ with $f(\mathbf{r}, t_0) \equiv 0$, and the function $f(\mathbf{r}, t)$ has partial derivatives till the order of $2M - 2$ to be continuous. The atomic units are applied throughout this paper. The normalization condition reads

$$\|\Psi\|^2 = \int |\Psi(\mathbf{r}, t)|^2 \,\mathrm{d}\mathbf{r} = 1, \qquad t \in [t_0, T]. \tag{29}$$

We rewrite the operators $\tilde{A}_k^{(M)}$ and $S_k^{(M)}$ in the form

$$\begin{aligned}
\tilde{A}_k^{(1)} &= H, & S_k^{(1)} &= 0,\\
\tilde{A}_k^{(2)} &= \tilde{A}_k^{(1)} + G^{(2)}, & S_k^{(2)} &= S_k^{(1)} + Z^{(2)},\\
\tilde{A}_k^{(3)} &= \tilde{A}_k^{(2)} + G^{(3)} - \frac{\tau^4}{720}\nabla_{\mathbf{r}}\left(\nabla_{\mathbf{r}}^2 \ddot{f}\right)\nabla_{\mathbf{r}}, & S_k^{(3)} &= S_k^{(2)} + Z^{(3)} + \frac{\tau^4}{720}\nabla_{\mathbf{r}}\left(\nabla_{\mathbf{r}}^2 \dot{f}\right)\nabla_{\mathbf{r}},
\end{aligned} \tag{30}$$

where the functions $G^{(l)}$ and $Z^{(l)}$ for $l = 2, 3$ read as

$$\begin{aligned}
G^{(2)} &= \frac{\tau^2}{24}\ddot{f},\\
Z^{(2)} &= \frac{\tau^2}{12}\dot{f},\\
G^{(3)} &= \frac{\tau^4}{1920}\dddot{f} + \frac{\tau^4}{1440}(\nabla_{\mathbf{r}}\dot{f})^2 - \frac{\tau^4}{720}(\nabla_{\mathbf{r}}\ddot{f})(\nabla_{\mathbf{r}}(U+f)) - \frac{\tau^4}{2880}\left(\nabla_{\mathbf{r}}^4\ddot{f}\right),\\
Z^{(3)} &= \frac{\tau^4}{480}\ddot{f} + \frac{\tau^4}{720}(\nabla_{\mathbf{r}}\dot{f})(\nabla_{\mathbf{r}}(U+f)) + \frac{\tau^4}{2880}\left(\nabla_{\mathbf{r}}^4\dot{f}\right),
\end{aligned} \tag{31}$$

and $f \equiv f(\mathbf{r}, t_c)$, $\dot{f} \equiv \partial_t f(\mathbf{r}, t)|_{t=t_c}, \ldots, U \equiv U(\mathbf{r})$. Below we put $M \leqslant 3$, since the considered schemes contain operator nabla with third order for implementation at $M \geqslant 4$.

3.1. The Kantorovich approach

In the close-coupling approximation, known in mathematics as the Kantorovich method [20, 41], the partial wavefunction $\Psi(\mathbf{r}, t)$ is expanded over the single-parameter basis functions $\{B_j(\Omega; r)\}_{j=1}^N$

$$\Psi(\mathbf{r}, t) = \sum_{j=1}^{N} B_j(\Omega; r)\chi_j(r, t). \tag{32}$$

In equation (32) the vector function $\boldsymbol{\chi}(r, t) = (\chi_1(r, t), \ldots, \chi_N(r, t))^T$ is unknown, and the components of the surface vector function $\mathbf{B}(\Omega; r) = (B_1(\Omega; r), \ldots, B_N(\Omega; r))^T$ form an orthonormal basis with respect to the set of angular coordinates Ω for each value of hyperradius r, which is treated here as a given parameter. In the Kantorovich approach [20, 41], the functions $B_j(\Omega; r) \in \mathcal{F}_r \sim \mathbf{L}_2(S^{d-1}(\Omega))$ are determined as solutions of the following parametric eigenvalue problem:

$$\left(-\frac{1}{2r^2}\hat{\mathbf{\Lambda}}_\Omega^2 + U(\mathbf{r})\right) B_j(\Omega; r) = E_j(r) B_j(\Omega; r), \tag{33}$$

where $\hat{\mathbf{\Lambda}}_\Omega^2$ is the generalized self-adjoint angular momentum operator, corresponding to the d-dimensional Laplace operator $\nabla_{\mathbf{r}}^2$. The eigenfunctions of this problem satisfy the same boundary conditions in angular variable Ω for $\Psi(\mathbf{r}, t)$ and are normalized as

$$\langle B_i(\Omega; r) \mid B_j(\Omega; r)\rangle_\Omega = \int \overline{B}_i(\Omega; r) B_j(\Omega; r)\, \mathrm{d}\Omega = \delta_{ij}, \tag{34}$$

where δ_{ij} is the Kronecker symbol.

After minimizing the Rayleigh–Ritz variational functional (see [20, 29]), and using the expansion (32) equation (27) is reduced to a set of N ordinary second-order differential equations

$$\mathrm{i}\mathbf{I}\frac{\partial \boldsymbol{\chi}(r, t)}{\partial t} = \mathbf{H}(r, t)\boldsymbol{\chi}(r, t), \qquad \boldsymbol{\chi}(r, t_0) = \boldsymbol{\chi}_0(r), \tag{35}$$

with

$$\mathbf{H}(r,t) = -\frac{1}{2r^{d-1}}\mathbf{I}\frac{\partial}{\partial r}r^{d-1}\frac{\partial}{\partial r} + \mathbf{V}(r,t) + \mathbf{Q}(r)\frac{\partial}{\partial r} + \frac{1}{r^{d-1}}\frac{\partial r^{d-1}\mathbf{Q}(r)}{\partial r}. \tag{36}$$

Here $\mathbf{I}$, $\mathbf{V}(r,t)$ and $\mathbf{Q}(r)$ are matrices of dimension $N \times N$, whose elements are given by the relation

$$V_{ij}(r,t) = V_{ji}(r,t) = \frac{E_i(r)+E_j(r)}{2}\delta_{ij} + \frac{1}{2}\left\langle \frac{\partial B_i(\Omega;r)}{\partial r}\middle| \frac{\partial B_j(\Omega;r)}{\partial r}\right\rangle_\Omega$$
$$+ \langle B_i(\Omega;r)|f(\mathbf{r},t)|B_j(\Omega;r)\rangle_\Omega, \qquad I_{ij} = \delta_{ij}, \tag{37}$$
$$Q_{ij}(r) = -Q_{ji}(r) = -\frac{1}{2}\left\langle B_i(\Omega;r)\middle|\frac{\partial B_j(\Omega;r)}{\partial r}\right\rangle_\Omega.$$

The boundary conditions have the form

$$\chi(0,t) = 0, \qquad \text{if} \quad \min_{1\leqslant j\leqslant N}\lim_{r\to 0} r^{d-1}|V_{jj}(r,t)| = \infty,$$
$$\lim_{r\to 0} r^{d-1}\left(\mathbf{I}\frac{\partial}{\partial r} - \mathbf{Q}(r)\right)\chi(r,t) = 0, \qquad \text{if} \quad \min_{1\leqslant j\leqslant N}\lim_{r\to 0} r^{d-1}|V_{jj}(r,t)| < \infty, \tag{38}$$
$$\lim_{r\to\infty}\chi(r,t) = 0.$$

The normalization condition reads

$$\int_0^\infty (\bar{\chi}(r,t))^T\,\chi(r,t)r^{d-1}\,\mathrm{d}r = 1. \tag{39}$$

In this case we obtain a finite $N \times N$ matrix operator-difference scheme for the unknown vector functions $\chi(r,t)$, similar to (25)

$$\tilde{\chi}_k^0 = \chi(r,t_k),$$
$$\left(\mathbf{I} - \frac{\overline{\alpha}_\eta^{(L)}\tilde{\mathbf{S}}_k^{(M)}}{2L}\right)\tilde{\chi}_k^{\eta/L} = \left(\mathbf{I} - \frac{\alpha_\eta^{(L)}\tilde{\mathbf{S}}_k^{(M)}}{2L}\right)\tilde{\chi}_k^{(\eta-1)/L}, \qquad \eta = 1,\ldots,L,$$
$$\hat{\chi}_k^0 = \tilde{\chi}_k^1,$$
$$\left(\mathbf{I} + \frac{\tau\overline{\alpha}_\zeta^{(M)}\tilde{\mathbf{A}}_k^{(M)}}{2M}\right)\hat{\chi}_k^{\zeta/M} = \left(\mathbf{I} + \frac{\tau\alpha_\zeta^{(M)}\tilde{\mathbf{A}}_k^{(M)}}{2M}\right)\hat{\chi}_k^{(\zeta-1)/M}, \qquad \zeta = 1,\ldots,M, \tag{40}$$
$$\tilde{\chi}_k^0 = \hat{\chi}_k^1,$$
$$\left(\mathbf{I} + \frac{\overline{\alpha}_\eta^{(L)}\tilde{\mathbf{S}}_k^{(M)}}{2L}\right)\tilde{\chi}_k^{\eta/L} = \left(\mathbf{I} + \frac{\alpha_\eta^{(L)}\tilde{\mathbf{S}}_k^{(M)}}{2L}\right)\tilde{\chi}_k^{(\eta-1)/L}, \qquad \eta = 1,\ldots,L,$$
$$\chi(r,t_{k+1}) = \tilde{\chi}_k^1.$$

Here the operators $\tilde{\mathbf{A}}_k^{(M)}$ and $\tilde{\mathbf{S}}_k^{(M)}$ for $M = 1,2,3$ have the form

$$\begin{aligned}
\tilde{\mathbf{A}}_k^{(1)} &= \mathbf{H}(r,t_c), & \tilde{\mathbf{S}}_k^{(1)} &= \mathbf{0},\\
\tilde{\mathbf{A}}_k^{(2)} &= \tilde{\mathbf{A}}_k^{(1)} + \tilde{\mathbf{G}}^{(2)}, & \tilde{\mathbf{S}}_k^{(2)} &= \tilde{\mathbf{S}}_k^{(1)} + \tilde{\mathbf{Z}}^{(2)},\\
\tilde{\mathbf{A}}_k^{(3)} &= \tilde{\mathbf{A}}_k^{(2)} + \tilde{\mathbf{G}}^{(3)} + \dot{\mathbf{C}}_k^{(3)}, & \tilde{\mathbf{S}}_k^{(3)} &= \tilde{\mathbf{S}}_k^{(2)} + \tilde{\mathbf{Z}}^{(3)} - \mathbf{C}_k^{(3)},
\end{aligned} \tag{41}$$

where $\tilde{\mathbf{G}}^{(l)}$ and $\tilde{\mathbf{Z}}^{(l)}$ are $N \times N$ matrices with elements given by the relations

$$\begin{aligned}
\tilde{G}_{ij}^{(l)} &= \tilde{G}_{ji}^{(l)} = \langle B_i(\Omega;r)|G^{(l)}|B_j(\Omega;r)\rangle_\Omega,\\
\tilde{Z}_{ij}^{(l)} &= \tilde{Z}_{ji}^{(l)} = \langle B_i(\Omega;r)|Z^{(l)}|B_j(\Omega;r)\rangle_\Omega.
\end{aligned} \tag{42}$$

The operator $\mathbf{C}_k^{(3)}$ is equal to zero for $\left(\nabla_{\mathbf{r}}^2 f\right) = 0$, otherwise it has the form

$$\mathbf{C}_k^{(3)} = \frac{\tau^4}{720}\left(-\frac{1}{r^{d-1}}\frac{\partial}{\partial r}r^{d-1}\tilde{\mathbf{D}}(r)\frac{\partial}{\partial r} + \tilde{\mathbf{V}}(r) - \tilde{\mathbf{Q}}^T(r)\frac{\partial}{\partial r} + \frac{1}{r^{d-1}}\frac{\partial r^{d-1}\tilde{\mathbf{Q}}(r)}{\partial r}\right), \tag{43}$$

where $\tilde{\mathbf{D}}(r)$, $\tilde{\mathbf{V}}(r)$ and $\tilde{\mathbf{Q}}(r)$ are $N \times N$ matrices with elements given by the relations

$$\begin{aligned}
\tilde{D}_{ij}(r) &= \tilde{D}_{ji}(r) = \langle B_i(\Omega; r)|\left(\nabla_{\mathbf{r}}^2 \dot{f}\right)|B_j(\Omega; r)\rangle_\Omega, \\
\tilde{V}_{ij}(r) &= \tilde{V}_{ji}(r) = \left\langle \frac{\partial B_i(\Omega; r)}{\partial r}\middle|\left(\nabla_{\mathbf{r}}^2 \dot{f}\right)\middle|\frac{\partial B_j(\Omega; r)}{\partial r}\right\rangle_\Omega + \frac{\tilde{X}_{ij}(r)}{r^2}, \\
\tilde{Q}_{ij}(r) &= -\langle B_i(\Omega; r)|\left(\nabla_{\mathbf{r}}^2 \dot{f}\right)\left|\frac{\partial B_j(\Omega; r)}{\partial r}\right\rangle_\Omega, \\
\tilde{X}_{ij}(r) &= \tilde{X}_{ji}(r) = \langle \hat{\mathbf{\Lambda}}_\Omega B_i(\Omega; r)|\left(\nabla_{\mathbf{r}}^2 \dot{f}\right)|\hat{\mathbf{\Lambda}}_\Omega B_j(\Omega; r)\rangle_\Omega.
\end{aligned} \tag{44}$$

Using equation (33), we obtain the simple form of $\tilde{X}_{ij}(r)$

$$\begin{aligned}
\tilde{X}_{ij}(r) &= \langle B_i(\Omega; r)|g(\mathbf{r})|B_j(\Omega; r)\rangle_\Omega, \\
g(\mathbf{r}) &= r^2[E_i(r) + E_j(r) - 2U(\mathbf{r})]\left(\nabla_{\mathbf{r}}^2 \dot{f}\right) + \tfrac{1}{2}\left(\hat{\mathbf{\Lambda}}_\Omega^2\left(\nabla_{\mathbf{r}}^2 \dot{f}\right)\right).
\end{aligned} \tag{45}$$

4. High-order approximation schemes of FEM

To solve the problem (35) on the time grid $\Omega_\tau[t_0, T]$, the boundary conditions (38) and normalization condition (39) with respect to the space variable r in an infinite interval are replaced with the appropriate conditions in a finite interval $\hat{\Omega}_r[r_{\min}, r_{\max}]$. Then at each step k of the time grid $\Omega_\tau[t_0, T]$ we consider a discrete representation of the solution $\chi(r, t_k)$ of the problem (35).

Now we cover the interval $\Delta = [r_{\min}, r_{\max}]$ by a set of n subintervals $\Delta_j = [r_{j-1}, r_j]$ in such a way that $\Delta = \bigcup_{j=1}^n \Delta_j$. In each subinterval Δ_j the nodes

$$r_{j,i}^p = r_{j-1} + \frac{h_j}{p}i, \qquad h_j = r_j - r_{j-1}, \qquad i = 0, \ldots, p, \tag{46}$$

and the Lagrange elements

$$\phi_{j,i}^p(r) = \prod_{l=0, l\neq i}^{p} \frac{\left(r - r_{j,l}^p\right)}{\left(r_{j,i}^p - r_{j,l}^p\right)} \tag{47}$$

are determined. By means of the Lagrange elements $\phi_{j,i}^p(r)$, we define a set of local functions $N_l(\rho)$ as follows:

$$N_l^p(r) = \begin{cases}
\begin{cases}\phi_{1,0}^p(r), & r \in \Delta_1, \\ 0, & r \notin \Delta_1,\end{cases} & l = 0, \\
\begin{cases}\phi_{j,i}^p(r), & r \in \Delta_j, \\ 0, & r \notin \Delta_j,\end{cases} & l = i + p(j-1), i = 1, \ldots, p-1, \\
\begin{cases}\phi_{j,p}^p(r), & r \in \Delta_j, \\ \phi_{j+1,0}^p(r), & r \in \Delta_{j+1}, \\ 0, & r \notin \Delta_j \bigcup \Delta_{j+1},\end{cases} & l = jp, j = 1, \ldots, n-1, \\
\begin{cases}\phi_{n,p}^p(r), & r \in \Delta_n, \\ 0, & r \notin \Delta_n,\end{cases} & l = np.
\end{cases} \tag{48}$$

The functions $\left\{N_l^p(r)\right\}_{l=0}^{L}$, $L = np$ form a basis in the space of polynomials of the order p. We approximate each function $\chi_\mu(r, t_k)$ by a finite sum of local functions $N_l^p(r)$

$$\chi_\mu(r, t_k) = \sum_{l=0}^{np} \chi_\mu^l(t_k) N_l^p(r), \qquad \mu = 1, \ldots, N, \tag{49}$$

where $\chi_\mu^l(t_k) \equiv \chi_\mu^l\left(r_{j,i}^p, t_k\right), l = i + p(j-1)$ are the node values of the unknown function $\chi_\mu(r, t_k)$, with respect to which the initial problem is numerically solved.

Substituting (49) into the operator-difference scheme (40), multiplying it from the left by $N_l^p(r)$ and integrating over the interval $\hat{\Omega}_r[r_{\min}, r_{\max}]$, the scheme (40) is reduced to a set of algebraic equations for $\boldsymbol{\chi}_k = \left\{\left\{\chi_\mu^l\left(r_{j,i}^p, t_k\right)\right\}_{l=0}^{np}\right\}_{\mu=1}^{N}$ at given M

$$\begin{aligned}
&\tilde{\boldsymbol{\chi}}_k^0 = \boldsymbol{\chi}_k,\\
&\left(\mathbf{B}^p - \frac{\overline{\alpha}_\eta^{(L)}}{2L}\mathbf{S}_k^p\right)\tilde{\boldsymbol{\chi}}_k^{\eta/L} = \left(\mathbf{B}^p - \frac{\alpha_\eta^{(L)}}{2L}\mathbf{S}_k^p\right)\tilde{\boldsymbol{\chi}}_k^{(\eta-1)/L}, \qquad \eta = 1, \ldots, L,\\
&\hat{\boldsymbol{\chi}}_k^0 = \tilde{\boldsymbol{\chi}}_k^1,\\
&\left(\mathbf{B}^p + \frac{\tau\overline{\alpha}_\zeta^{(M)}}{2M}\mathbf{A}_k^p\right)\hat{\boldsymbol{\chi}}_k^{\zeta/M} = \left(\mathbf{B}^p + \frac{\tau\alpha_\zeta^{(M)}}{2M}\mathbf{A}_k^p\right)\hat{\boldsymbol{\chi}}_k^{(\zeta-1)/M}, \qquad \zeta = 1, \ldots, M,\\
&\tilde{\boldsymbol{\chi}}_k^0 = \hat{\boldsymbol{\chi}}_k^1,\\
&\left(\mathbf{B}^p + \frac{\overline{\alpha}_\eta^{(L)}}{2L}\mathbf{S}_k^p\right)\tilde{\boldsymbol{\chi}}_k^{\eta/L} = \left(\mathbf{B}^p + \frac{\alpha_\eta^{(L)}}{2L}\mathbf{S}_k^p\right)\tilde{\boldsymbol{\chi}}_k^{(\eta-1)/L}, \qquad \eta = 1, \ldots, L,\\
&\boldsymbol{\chi}_{k+1} = \tilde{\boldsymbol{\chi}}_k^1.
\end{aligned} \tag{50}$$

The matrices $\mathbf{A}_k^p$, $\mathbf{B}^p$ and $\mathbf{S}_k^p$ are symmetric and possess the band structure. The matrix $\mathbf{B}^p$ is positive definite. They have the following form:

$$\mathbf{A}_k^p = \sum_{j=1}^{n} \mathbf{a}_{j,k}^p, \qquad \mathbf{B}^p = \sum_{j=1}^{n} \mathbf{b}_j^p, \qquad \mathbf{S}_k^p = \sum_{j=1}^{n} \mathbf{s}_{j,k}^p, \tag{51}$$

where the local matrices $\mathbf{a}_{j,k}^p$, $\mathbf{b}_j^p$ and $\mathbf{s}_{j,k}^p$ are calculated similar to [20]. As is known [26], the theoretical estimate in the norm $\|\cdot\|$ on the finite-element grid for the difference between the exact solution $\boldsymbol{\chi}(r, t_k)$ and the approximate one $\boldsymbol{\chi}_k$ has the order $\|\boldsymbol{\chi}(r, t_k) - \boldsymbol{\chi}_k\| = O(h^{p+1})$, where h is the maximal step of the finite-element grid.

To analyze the convergence on a sequence of three double-crowding time grids, we define the auxiliary time-dependent discrepancy functions

$$Er^2(t, j) = \sum_{\nu=1}^{N} \int_0^{r_{\max}} \left|\chi_\nu(r, t) - \chi_\nu^{\tau_j}(r, t)\right|^2 r^{d-1}\, \mathrm{d}r, \qquad j = 1, 2, 3, \tag{52}$$

and the Runge coefficient

$$\beta(t) = \log_2 \left|\frac{Er(t, 1) - Er(t, 2)}{Er(t, 2) - Er(t, 3)}\right|, \tag{53}$$

where $\chi_\nu^{\tau_j}(r, t)$ are the numerical solutions obtained with the time step $\tau_j = \tau/2^{j-1}$. For the function $\chi_\nu(r, t)$ one can use the numerical solution obtained with the time step $\tau_4 = \tau/8$. Hence, we will obtain the numerical estimates for the convergence order of the numerical scheme (50), which strongly correspond to theoretical ones $\beta(t) \equiv \beta_M(t) \approx 2M$.

From the estimation (26) of the above theorem it follows that the estimation for steps $\tau = \tau_M < 1$ of the numerical scheme (50) with $M = 1, 2, 3$ has the same bound for ϵ_M with $M = 1, 2$ as at fixed error ϵ_3 under the conditions

$$\tau_1 = \tau_3^3, \qquad \tau_2 = \sqrt{\tau_3^3}. \tag{54}$$

In each transformation of $\Psi(t_k)$ into $\Psi(t_{k+1})$ we obtained one-, four- and five-layer schemes for $M = 1, 2$ and 3, respectively, hence, for $M = 2, 3$ the computer time consumption was approximately four and five times greater than for $M = 1$. However, for the time steps (54) and $M = 1, 2$ the required total computational time will be approximately $1/\left(5\tau_3^2\right)$ and $4/(5\sqrt{\tau_3})$ times greater than that for $M = 3$, respectively.

5. Benchmark calculations

5.1. The exactly solvable one-dimensional model

The TDSE for a one-dimensional harmonic oscillator with explicitly time-dependent frequency in the finite time interval $t \in [0, T]$ has the form

$$\mathrm{i}\frac{\partial\psi(x,t)}{\partial t} = \left(-\frac{1}{2}\frac{\partial^2}{\partial x^2} + \frac{\omega^2(t)x^2}{2}\right)\psi(x,t), \qquad \psi_0(x) = \sqrt[4]{\frac{1}{\pi}}\exp\left(-\frac{1}{2}(x-\sqrt{2})^2\right), \tag{55}$$

with $\omega^2(t) = 4 - 3\exp(-t)$ [23]. The exact solution of Cauchy problem (55) reads as

$$\psi_{\mathrm{ext}}(x,t) = \sqrt[4]{\frac{1}{\pi}}\exp(-X(t)x^2 + 2Y(t)x - Z(t)), \tag{56}$$

where the functions $X(t)$, $Y(t)$ and $Z(t)$ satisfy the Cauchy problem

$$\begin{aligned}
&\mathrm{i}\frac{\mathrm{d}}{\mathrm{d}t}X(t) = 2X^2(t) - \frac{\omega^2(t)}{2}, && X(0) = \frac{1}{2},\\
&\mathrm{i}\frac{\mathrm{d}}{\mathrm{d}t}Y(t) = 2X(t)Y(t), && Y(0) = \frac{\sqrt{2}}{2},\\
&\mathrm{i}\frac{\mathrm{d}}{\mathrm{d}t}Z(t) = -X(t) + 2Y^2(t), && Z(0) = 1.
\end{aligned} \tag{57}$$

To approximate the solution $\psi(x,t)$ in the variable x, we make use of the finite-element grid $\hat{\Omega}_x[x_{\min}, x_{\max}] = \{x_{\min} = -10, (100), x_{\max} = 10\}$ and the time step $\tau = 0.009\,765\,625$, where the number in the brackets denotes the number of finite element in the intervals. Between each two nodes we apply the Lagrange interpolation polynomials up to the order $p = 8$. Figure 1 displays the behavior of discrepancy functions $Er(t; j)$, $j = 1, 2, 3$ (dash-dotted, dashed and solid curves) and convergence rate $\beta_M(t)$ for the approximations of the order $2M = 2, 4, 6$ that strongly correspond to theoretical ones.

5.2. The exactly solvable two-dimensional model

The TDSE for a two-dimensional oscillator (or a charged particle in the time-independent uniform magnetic field) subject to the external governing electric field with the components $\mathcal{E}_1(t)$ and $\mathcal{E}_2(t)$ nonzero in the finite time interval $t \in [0, T]$ has the form [7]

$$\begin{aligned}
\mathrm{i}\frac{\partial}{\partial t}\phi(x_1, y_1, t) = \Bigg(&-\frac{1}{2}\left(\frac{\partial^2}{\partial x_1^2} + \frac{\partial^2}{\partial y_1^2}\right) + \frac{\mathrm{i}\omega}{2}\left(x_1\frac{\partial}{\partial y_1} - y_1\frac{\partial}{\partial x_1}\right)\\
&+ \frac{\omega^2}{8}\left(x_1^2 + y_1^2\right) - x_1\mathcal{E}_1(t) - y_1\mathcal{E}_2(t)\Bigg)\phi(x_1, y_1, t).
\end{aligned} \tag{58}$$

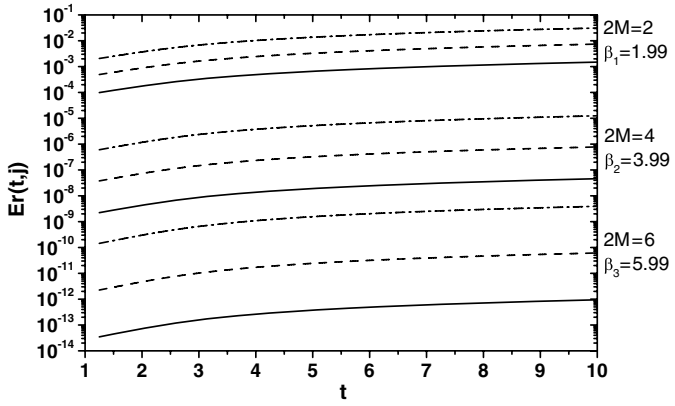

Figure 1. The test results of the discrepancy functions $Er(t, j)$, $j = 1, 2, 3$ (dash-dotted, dashed and solid curves) for the approximations of the order $2M = 2, 4, 6$ with the time step $\tau = 0.009\,765\,625$.

Here we suppose the dipole approximation to be valid and use the atomic units. The transformation to a coordinate system rotating with the frequency $\omega/2$

$$x_1 = x\cos\left(\frac{\omega t}{2}\right) + y\sin\left(\frac{\omega t}{2}\right), \qquad y_1 = y\cos\left(\frac{\omega t}{2}\right) - x\sin\left(\frac{\omega t}{2}\right) \tag{59}$$

leads to the following equation:

$$\mathrm{i}\frac{\partial}{\partial t}\phi(x, y, t) = \left(-\frac{1}{2}\left(\frac{\partial^2}{\partial x^2} + \frac{\partial^2}{\partial y^2}\right) + \frac{\omega^2}{8}(x^2 + y^2) + f_1(t)x + f_2(t)y\right)\phi(x, y, t), \tag{60}$$

where

$$\begin{aligned} f_1(t) &= -\mathcal{E}_1(t)\cos\left(\frac{\omega t}{2}\right) + \mathcal{E}_2(t)\sin\left(\frac{\omega t}{2}\right), \\ f_2(t) &= -\mathcal{E}_1(t)\sin\left(\frac{\omega t}{2}\right) - \mathcal{E}_2(t)\cos\left(\frac{\omega t}{2}\right). \end{aligned} \tag{61}$$

In the polar coordinates (r, θ) this equation has the form

$$\begin{aligned} \mathrm{i}\frac{\partial}{\partial t}\phi(r, \theta, t) = \Bigg(&-\frac{1}{2}\left(\frac{1}{r}\frac{\partial}{\partial r}r\frac{\partial}{\partial r} + \frac{1}{r^2}\frac{\partial^2}{\partial\theta^2}\right) \\ &+ \frac{\omega^2 r^2}{8} + r(f_1(t)\cos(\theta) + f_2(t)\sin(\theta))\Bigg)\phi(r, \theta, t). \end{aligned} \tag{62}$$

Using the Galerkin projection of the solutions onto the basis of angular functions $B_j(\theta)$

$$\phi(r, \theta, t) = \sum_{j=1}^{N} B_j(\theta)\chi_j(r, t), \tag{63}$$

where

$$B_1(\theta) = \frac{1}{\sqrt{2\pi}}, \qquad B_{2j}(\theta) = \frac{\sin(j\theta)}{\sqrt{\pi}}, \qquad B_{2j+1}(\theta) = \frac{\cos(j\theta)}{\sqrt{\pi}}, \quad j \geqslant 1, \tag{64}$$

we arrive at the matrix equation (35) for the unknown coefficients $\{\chi_j(r,t)\}_{j=1}^N$ in the interval $t \in [0, T]$. The initial functions $\chi_j(r,t)$ at $t = 0$ (in the case $f_1(0) = f_2(0) = 0$) are chosen in the form

$$\chi_j(r,0) = \sqrt{\omega}\exp\left(-\tfrac{1}{4}\omega r^2\right)\delta_{j1}, \tag{65}$$

that corresponds to the ground state wave packet of the free oscillator

$$\phi_0(x,y) = \sqrt{\frac{\omega}{2\pi}}\exp\left(-\frac{\omega}{4}(x^2+y^2)\right). \tag{66}$$

The exact solution of equation (60) reads with the initial condition (66) as

$$\begin{aligned}\phi_{\rm ext}(x,y,t) = &\sqrt[4]{\frac{\omega}{2\pi}}\exp(-X_1(t)x^2 + 2Y_1(t)x - Z_1(t))\\ &\times\sqrt[4]{\frac{\omega}{2\pi}}\exp(-X_2(t)y^2 + 2Y_2(t)y - Z_2(t)),\end{aligned} \tag{67}$$

where the functions $X_j(t)$, $Y_j(t)$, $Z_j(t)$, $j = 1, 2$ satisfy the Cauchy problem

$$\begin{aligned}&\mathrm{i}\frac{\mathrm{d}}{\mathrm{d}t}X_j(t) = 2X_j^2(t) - \frac{\omega^2}{8}, && X_j(0) = \frac{\omega}{4},\\ &\mathrm{i}\frac{\mathrm{d}}{\mathrm{d}t}Y_j(t) = 2X_j(t)Y_j(t) + \frac{f_j(t)}{2}, && Y_j(0) = 0,\\ &\mathrm{i}\frac{\mathrm{d}}{\mathrm{d}t}Z_j(t) = -X_j(t) + 2Y_j^2(t), && Z_j(0) = 0.\end{aligned} \tag{68}$$

Here the exact solution of the first differential equation reads $X_j(t) \equiv \omega/4$ in the whole time interval $t \in [0, T]$.

Note that this problem has an analytical solution for the particular choice of the field $\mathcal{E}_j(t) = a_j \sin(\omega_j t)$ which provides a good test example to examine the efficiency of numerical algorithms and the rate of convergence of the projection with respect to the number N of radial equations and time T. The necessary projections of the exact solution have the form

$$\chi_j^{\rm ext}(r,t) = \int_0^{2\pi} B_j(\theta)\phi_{\rm ext}(r,\theta,t)\,\mathrm{d}\theta. \tag{69}$$

We choose $\omega = 4\pi, \omega_1 = 3\pi, \omega_2 = 5\pi, a_1 = 24$ and $a_2 = 9$. For these parameters the absolute value of the solution $\phi(r,\theta,t)$ should be periodical with the period $T = 2$.

To approximate the solution $\chi_j(r,t)$ in the variable r, we use the finite-element grid $\hat{\Omega}_r[r_{\min}, r_{\max}] = \{r_{\min} = 0, (120), 1.5, (60), r_{\max} = 4\}$ and the time step $\tau = 0.0125$, where the number in the brackets denotes the number of finite elements in the intervals. Between each two nodes we apply the Lagrange interpolation polynomials up to the order $p = 8$.

Figure 2 displays the behavior of the discrepancy functions $Er(t; j)$, $j = 1, 2, 3$ (dash-dotted, dashed and solid curves) and convergence rate $\beta_M(t)$ for the approximations of the order $2M = 2, 4, 6$ at $N = 20$ (a) and $N = 30$ (b) that strongly correspond to theoretical ones. In figure 3, the absolute values of the numerical solution $\phi(x,y,t)$ and the difference $\phi_{\rm ext}(x,y,t) - \phi(x,y,t)$ are shown at $t = 1.2$ and $t = 2$. Here $N = 20$, $\tau_4 = \tau/8 = 0.001\,5625$ and $M = 3$. In figure 4 only the differences are shown at $N = 30$.

The key result that follows from the above analysis is that the required number N of angular basis functions can be controlled by solving not only the stationary Schrödinger equation [30], but also the exact solvable TDSE. Such benchmark calculations open the opportunity to control the moving spatial region covered by the time-dependent wave packet, expanded over the angular basis.

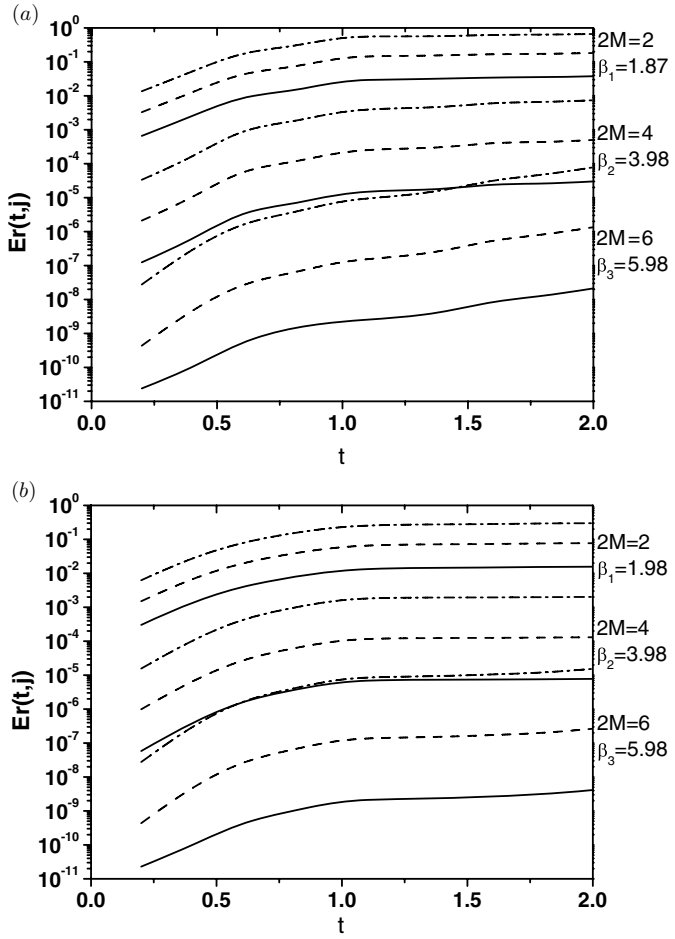

Figure 2. The test results of the discrepancy functions $Er(t, j)$, $j = 1, 2, 3$ (dash-dotted, dashed and solid curves) for the approximations of the order $2M = 2, 4, 6$ with the time step $\tau_4 = \tau/8 = 0.001\,5625$ at $N = 20$ (a) and $N = 30$ (b).

If the initial state of a free harmonic oscillator is taken to be a Gaussian wave packet, differing in width from the ground eigenstate, then the evolution consists in periodic oscillations of the packet width, i.e. repeated focusing and defocusing in the coordinate and momentum space. Similar behavior is observed in Gaussian light beams in parabolic gradient waveguides (see, e.g., [42] and references therein). Recently this oscillator property was discussed in relation to the problem of channeling and super-focusing of light nuclear beams in thin doped films [43].

We calculated the time dependence of the wave packet shape in the model of a two-dimensional oscillator driven by an external field. Figure 5 shows the temporal dynamics of the closed loop in the x, y plane, within which the probability density $|\phi(x, y, t)|^2$ is not less than one half of its maximal value at given t. For calculations we took the frequencies to be the same as above and considered two cases: $a_1 = a_2 = 0$ (a), and $a_1 = 24$, $a_2 = 9$ (b). In both cases the wavefunction at the initial moment of time was $\phi_0(x, y) = \sqrt{\omega/(20\pi)}\exp(-\omega(x^2 + y^2)/40)$.

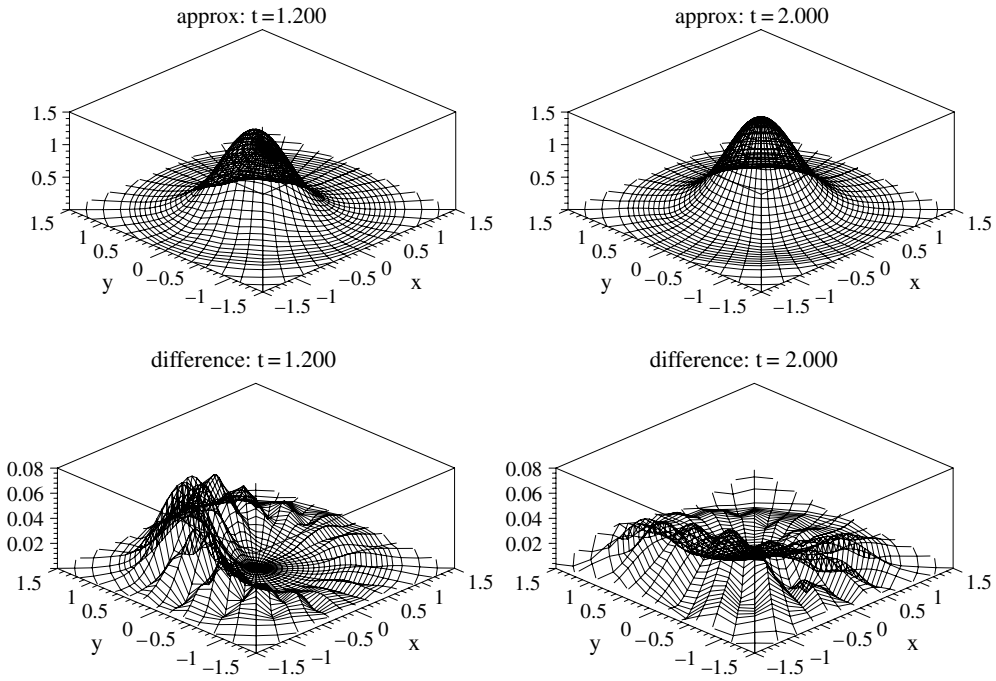

Figure 3. The absolute values of the numerical solution $\phi(x, y, t)$ and differences $\phi_{\text{ext}}(x, y, t) - \phi(x, y, t)$ at $t = 1.2$ and $t = 2$. Here $N = 20$, $\tau_4 = \tau/8 = 0.001\,5625$ and $M = 3$.

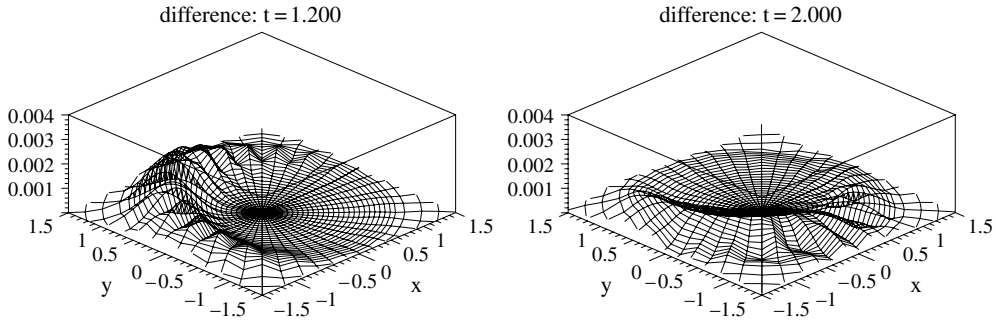

Figure 4. The differences $\phi_{\text{ext}}(x, y, t) - \phi(x, y, t)$ at the same conditions as in figure 3 except $N = 30$.

Periodical restoration of the initial wave packet shape (66) is seen to occur, wherever the packet center is at rest (a) or rotating (b).

5.3. The inexactly solvable three-dimensional model

The δ-kicks is a widely used approximation for the electric-field pulses that are much shorter than the classical orbital period [4, 5, 44–49]. The Hamiltonian of a kicked hydrogen atom in

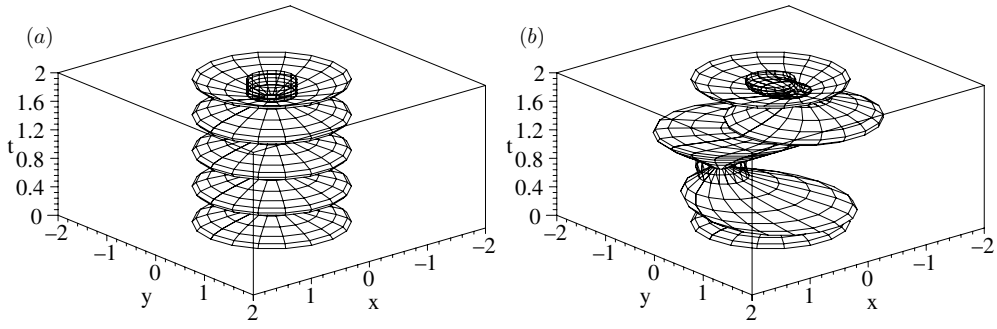

Figure 5. Temporal dynamics of the loop in the x, y plane within which the probability density $|\phi(x, y, t)|^2$ is greater than one half of its maximal value, i.e. $|\phi(x, y, t)|^2 \geqslant \max_{x,y} |\phi(x, y, t)|^2/2$.

the presence of a constant magnetic field parallel to the z-axis is given by

$$H(\mathbf{r}, t) = H_0(\mathbf{r}) + V_{\text{ext}}(t), \qquad H_0(\mathbf{r}) = -\frac{1}{2}\Delta_{\mathbf{r}} - \frac{1}{r} + V_Z(\mathbf{r}),$$
$$V_{\text{ext}}(t) = \sum_{s=1}^{S} \mathbf{r}\mathbf{F}_s \delta(t - sT), \tag{70}$$

where S is the number of kicks, T is the period of kicks and $\mathbf{F}_s$ is the amplitude of the sth kick. The term $V_Z(\mathbf{r})$ accounts for the interaction of an atom with magnetic field [50]

$$V_Z(\mathbf{r}) = \tfrac{1}{8}\gamma^2 r^2 \sin^2(\theta), \tag{71}$$

where γ is the strength of the magnetic field.

We consider the model of unidirectional kicks (which is true, e.g., in the case of half-cycle pulses [44]) and assume the electric field to be directed along the z-axis, so that $\mathbf{r}\mathbf{F}_s = zF_s$. Therefore, the z-component of the orbital angular momentum is conserved and m is a good quantum number. Further, it is convenient to work with parabolic states. If the magnetic field is absent ($\gamma = 0$), we make use of the following orthogonal relation between the parabolic states and (n, l, m) eigenstates:

$$\Phi^{(0)}_{n_1 n_2 m}(\mathbf{r}) = \sum_{l=|m|}^{n-1} A^{n_1 n_2}_{nlm} \Phi^{(0)}_{nlm}(\mathbf{r}), \qquad \Phi^{(0)}_{nlm}(\mathbf{r}) = \sum_{n_1, n_2 = 0}^{n-|m|} A^{n_1 n_2}_{nlm} \Phi^{(0)}_{n_1 n_2 m}(\mathbf{r}). \tag{72}$$

Here $n = n_1 + n_2 + |m| + 1$ is the principal quantum number, and the matrix elements $A^{n_1 n_2}_{nlm}$ are given in [51, 52]. In the presence of a magnetic field the initial state $\psi_0(\mathbf{r})$ is an eigenfunction of the Hamiltonian $H_0(\mathbf{r})$. In weak magnetic fields this state can also be specified by the principal quantum number n.

In the interval between the $(s-1)$ th and sth kicks the atom evolves freely according to the TDSE

$$\mathrm{i}\frac{\partial \psi(\mathbf{r}, t)}{\partial t} = H_0(\mathbf{r})\psi(\mathbf{r}, t), \qquad \psi(\mathbf{r}, t) \in \mathbf{W}^1_2(\mathbf{R}^3 \otimes ((s-1)T_+, sT_-)), \tag{73}$$

where $T_\pm = T \pm 0$. To illustrate the computational algorithm for periodic δ-kicks, we consider the Schrödinger equation for a single kick at the moment time $t = sT$:

$$\mathrm{i}\frac{\partial \psi(\mathbf{r}, t)}{\partial t} = (H_0 + zF_s\delta(t - sT))\psi(\mathbf{r}, t), \qquad \psi(\mathbf{r}, t) \in \mathbf{W}^1_2(\mathbf{R}^3 \otimes (sT_-, sT_+)). \tag{74}$$

The case of sequential kicks is then treated by repeating the computational steps for a single kick. Thus, the same method also allows one to handle the cases of non-periodic and non-equal kicks as well as of alternating kicks.

We calculate the wavefunction $\psi(\mathbf{r}, sT_+)$ immediately after the kick ($t = sT_+$) using the following formula:

$$\psi(\mathbf{r}, sT_+) = \exp\left(-\mathrm{i}H_0(\mathbf{r})(sT_+ - sT_-) - \mathrm{i}zF_s \int_{sT_-}^{sT_+} \delta(t - sT)\,\mathrm{d}t\right)\psi(\mathbf{r}, sT_-), \tag{75}$$

where $\psi(\mathbf{r}, sT_-)$ is the wavefunction right before the kick ($t = sT_-$). Note that $sT_+ - sT_- \to 0$ and $\int_{sT_-}^{sT_+} \delta(t - sT)\,\mathrm{d}t \equiv 1$. Consequently, equation (75) is equivalent to the formula [53]

$$\psi(\mathbf{r}, sT_+) = \exp(-\mathrm{i}zF_s)\,\psi(\mathbf{r}, sT_-). \tag{76}$$

Performing the scaling transformations $\tilde{r} = r/n, \tilde{t} = t/n^2$ and $\tilde{T} = T/n^2$ in equation (27) with the Hamiltonian (70) and making use of the Kantorovich expansion of the solutions over the orthogonal basis of functions $B_j(\eta = \cos(\theta); r)$

$$\psi(\tilde{\mathbf{r}}, \tilde{t}) = \frac{\exp(\mathrm{i}m\varphi)}{\sqrt{2\pi}} \sum_{j=1}^{N} B_j(\eta; \tilde{r})\chi_j(\tilde{r}, \tilde{t}), \tag{77}$$

we arrive at the matrix equation (35) for unknown coefficients $\{\chi_j(\tilde{r}, \tilde{t})\}_{j=1}^N$ in the interval $t \in [0, S\tilde{T}]$. The functions $B_j(\eta; r)$ are solutions of the following one parametric eigenvalue problem [11, 30]:

$$\left(-\frac{\partial}{\partial\eta}(1-\eta^2)\frac{\partial}{\partial\eta} + \frac{m^2}{1-\eta^2} - 2n\tilde{r} + \frac{\gamma^2 n^4 \tilde{r}^4}{4}(1-\eta^2)\right)B_j(\eta; \tilde{r}) = 2\tilde{r}^2 E_j(\tilde{r})B_j(\eta; \tilde{r}). \tag{78}$$

Using the scheme (50) in the time interval $((s-1)T_+, sT_-)$, we get a set of equations

$$\begin{aligned}
&\hat{\chi}_k^0 = \chi_k,\\
&\left(\mathbf{B}^p + \frac{\tau\overline{\alpha}_\zeta^{(M)}}{2M}\mathbf{A}_k^p\right)\hat{\chi}_k^{\zeta/M} = \left(\mathbf{B}^p + \frac{\tau\alpha_\zeta^{(M)}}{2M}\mathbf{A}_k^p\right)\hat{\chi}_k^{(\zeta-1)/M}, \qquad \zeta = 1, \ldots, M,\\
&\chi_{k+1} = \hat{\chi}_k^1.
\end{aligned} \tag{79}$$

In practical calculation of kicks we used the approximate procedure similar to equation (79)

$$\begin{aligned}
&\hat{\chi}_{sT}^0 = \chi_{sT_-},\\
&\left(\mathbf{B}^p + \frac{\overline{\alpha}_\zeta^{(M)}}{2M}\mathbf{D}_{sT}^p\right)\hat{\chi}_{sT}^{\zeta/M} = \left(\mathbf{B}^p + \frac{\alpha_\zeta^{(M)}}{2M}\mathbf{D}_{sT}^p\right)\hat{\chi}_{sT}^{(\zeta-1)/M}, \qquad \zeta = 1, \ldots, M,\\
&\chi_{sT_+} = \hat{\chi}_{sT}^1,
\end{aligned} \tag{80}$$

which conserves the unitarity and is correct up to the order $O\left(\|F_s z\|^{2M}_{L_2(S_+^2 \otimes [\tilde{r}_{\min}, \tilde{r}_{\max}])}\right)$. Here the symmetric banded matrix $\mathbf{D}_{sT}^p$ is determined by the longitudinal dipole matrix elements [11, 30]. Such procedure retains the same order of approximation as in the case of free evolution (79) and, as shown below, facilitates efficient treatment of the momentum shift operator $\exp(\mathrm{i}zF_s)$.

To calculate the dependence of the solutions $\{\chi_j(\tilde{r}, \tilde{t})\}_{j=1}^N$ upon the spatial variable $\tilde{r}$ in the finite interval $[\tilde{r}_{\min}, \tilde{r}_{\max}]$, we introduced the finite-element grid $\hat{\Omega}_{\tilde{r}}[\tilde{r}_{\min}, \tilde{r}_{\max}] = \{\tilde{r}_{\min} = 0, (50), 10, (100), \tilde{r}_{\max} = 80\}$. Between each two nodes of the grid the Lagrange interpolation polynomials of the order $p = 8$ have been applied.

Table 3 displays the discrepancy functions $Er(t; j)$, $j = 1, 2, 3$, and the convergence rate $\beta_M(t)$ for the approximations of the order $2M = 2$ ($\tilde{\tau} = \tilde{T}/64$), $2M = 4$ ($\tilde{\tau} = \tilde{T}/16$)

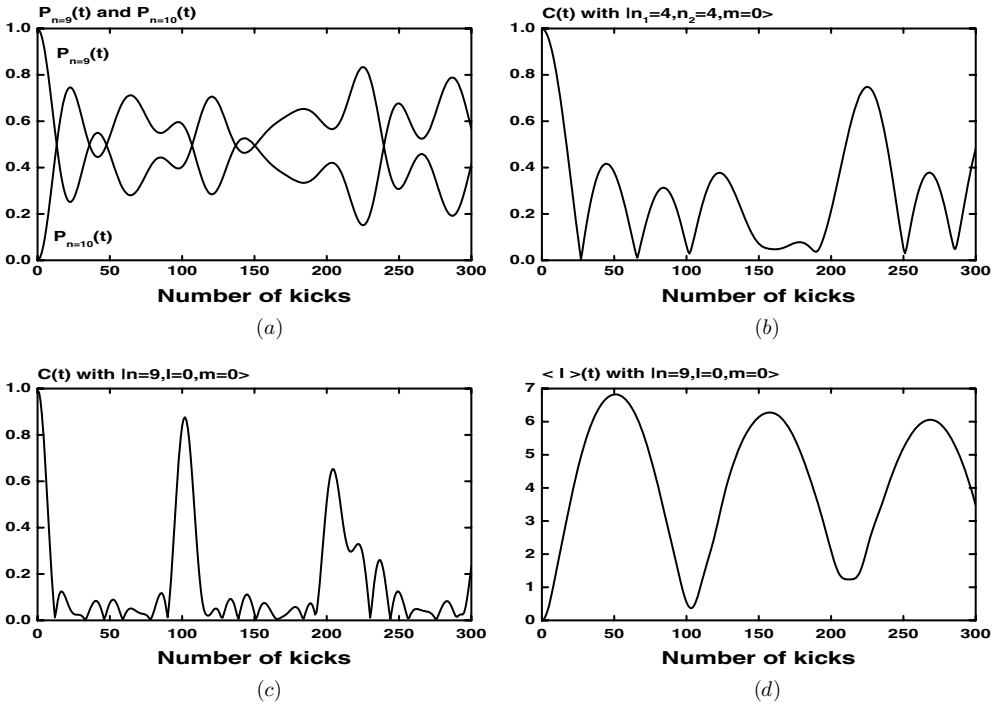

Figure 6. The dynamics of physical quantities of a kicked hydrogen atom. Comments are given in the text.

and $2M = 6$ ($\tilde{\tau} = \tilde{T}/8$) at the moment time $t = sT_+$ ($s = 1, \ldots, 6$) for the initial Zeeman vibrational state $|n = 5, v = 0, m = 0\rangle$ which corresponds to the minimal energy within the $n = 5$ manifold. Here $T = 1028$, $F = 2 \times 10^{-3}$, $\gamma = 1.472 \times 10^{-5}$ and $N = 10$. As evident from the table 3, though the time steps $\tilde{\tau}$ for schemes with $M = 2$ and $M = 3$ are bigger than for scheme with $M = 1$, these schemes provide considerably best accuracy. However, the convergence rates $\beta_M(t)$ corresponding to their theoretical estimations are achieved only for the special choice time steps $\tilde{\tau}$ of the time grids, since the wave packet discontinues first order. Using equation (76) at $|\mathbf{rF}| < 1$, we have the following estimation for the difference of solutions $\|\psi(\mathbf{r}, sT_+) - \psi(\mathbf{r}, sT_-)\|$ at $T_+ - T_- \to 0$:

$$\|\psi(\mathbf{r}, sT_+) - \psi(\mathbf{r}, sT_-)\|^2 = 4 \int \mathrm{d}\mathbf{r} \sin^2\left(\frac{\mathbf{Fr}}{2}\right) |\psi(\mathbf{r}, sT_-)|^2 \approx O(F^2). \tag{81}$$

Therefore already after first kick at the moment time $t = T$ for the decreasing time step $\tilde{\tau}$ of the time grids, the coefficient Runge $\beta_M(t)$ should tend to unity, if the condition

$$\tilde{F} \leqslant (\tilde{\tau}/8)^{2M} \tag{82}$$

fails according to estimation (16). This fact was checked out by the performed additional numerical experiments. The time steps $\tilde{\tau} = 0.6425, 2.57, 5.14$ at $M = 1, 2, 3$ that were used in the above numerical experiments satisfied to the condition (82), which correspondingly comparable with $8\sqrt[2M]{\tilde{F}} = 0.8, 2.53, 3.71$ at scaled values $\tilde{F} = 10^{-2}$ and $\tilde{T} = 41.12$.

Employing the sixth-order implicit scheme for $\gamma = 0$, we performed the calculations for the same situation as in [4, 5], where the evolution of the initial parabolic state $|n_1 = 4, n_2 = 4, m = 0\rangle$ and spherical state $|n = 9, l = 0, m = 0\rangle$ in a train of kicks with

Table 2. The eigenvalues $E_{\rm calc}$ of the Zeeman states $|n = 9, v = 0, \ldots, n-1, m = 0\rangle$ of a hydrogen atom in the uniform magnetic field $\gamma = 1.472 \times 10^{-5}$ calculated for a set of $l = 0, \ldots, 8$ spherical functions, $\delta E_{\rm calc} = 8(E_{\rm calc} - E^{(0)})/\gamma^2$ agrees with the first-order correction $E^{(1)}_{pt}$ of the perturbation theory, $E_{pt} = E^{(0)} + \gamma^2 E^{(1)}_{pt}/8$. The notation (-3) means multiplication by 10^{-3}.

v	$E_{\rm calc}$	E^0	$\delta E_{\rm calc}$	$E^{(1)}_{pt}$
0	−6.172 798(−3)	−6.172 839 (−3)	1529.11	1529.16
1	−6.172 797(−3)	−6.172 839 (−3)	1545.01	1545.04
2	−6.172 747(−3)	−6.172 839 (−3)	3384.07	3384.10
3	−6.172 728(−3)	−6.172 839 (−3)	4080.42	4080.47
4	−6.172 689(−3)	−6.172 839 (−3)	5536.15	5536.38
5	−6.172 641(−3)	−6.172 839 (−3)	7315.02	7315.33
6	−6.172 582(−3)	−6.172 839 (−3)	9476.34	9476.83
7	−6.172 514(−3)	−6.172 839 (−3)	12006.50	12007.13
8	−6.172 435(−3)	−6.172 839 (−3)	14902.72	14903.51

Table 3. The discrepancy functions $Er(sT_+, j)$, $j = 1, 2, 3$ and the Runge coefficient $\beta_M(sT_+)$ for the approximations of the order $2M = 2, 4, 6$. Here $N = 10$, $T = 1028$, $F = 2 \times 10^{-3}$ and $\gamma = 1.472 \times 10^{-5}$. The notation (-x) means multiplication by 10^{-x}.

s	$Er(sT_+, 1)$	$Er(sT_+, 2)$	$Er(sT_+, 3)$	$\beta_1(sT_+)$
		$M = 1$		
1	0.1712(−0)	0.4129(−1)	0.8282(−2)	1.977
2	0.3414(−0)	0.8263(−1)	0.1663(−1)	1.971
3	0.5091(−0)	0.1240(−0)	0.2503(−1)	1.960
4	0.6727(−0)	0.1653(−0)	0.3334(−1)	1.943
5	0.8306(−0)	0.2063(−0)	0.4158(−1)	1.922
6	0.9818(−0)	0.2470(−0)	0.4983(−1)	1.898
		$M = 2$		
1	0.7031(−1)	0.4731(−2)	0.2835(−3)	3.882
2	0.1408(−0)	0.9708(−2)	0.1439(−2)	3.987
3	0.2117(−0)	0.1482(−1)	0.2771(−2)	4.030
4	0.2820(−0)	0.1970(−1)	0.2972(−2)	3.971
5	0.3509(−0)	0.2434(−1)	0.2258(−2)	3.886
6	0.4187(−0)	0.2890(−1)	0.2162(−2)	3.866
		$M = 3$		
1	0.4495(−1)	0.8613(−3)	0.1391(−4)	5.701
2	0.9069(−1)	0.2552(−2)	0.1465(−2)	6.342
3	0.1372(−0)	0.4912(−2)	0.2230(−2)	5.625
4	0.1829(−0)	0.6570(−2)	0.1450(−2)	5.106
5	0.2265(−0)	0.7236(−2)	0.1434(−2)	5.240
6	0.2695(−0)	0.7775(−2)	0.1380(−2)	5.355

the period $T = 5357$ and the strength $F \equiv F_s = 2 \times 10^{-3}$ was investigated. In accordance with $T_n = 2\pi/[1/2n^2 - 1/2(n+1)^2]$ the period $T = 5357$ corresponds to a resonance regime between the two states with $n = 9$ and $n = 10$, respectively. In this case the expectation value of the Hamiltonian $\langle\psi(\mathbf{r}, t)|H_0(\mathbf{r})|\psi(\mathbf{r}, t)\rangle$ at the time interval $t \in ((s-1)T_+, sT_-)$, has a lower bound, namely, the eigenvalue $E_n = -1/2n^2$ of the ground state of the free Hamiltonian

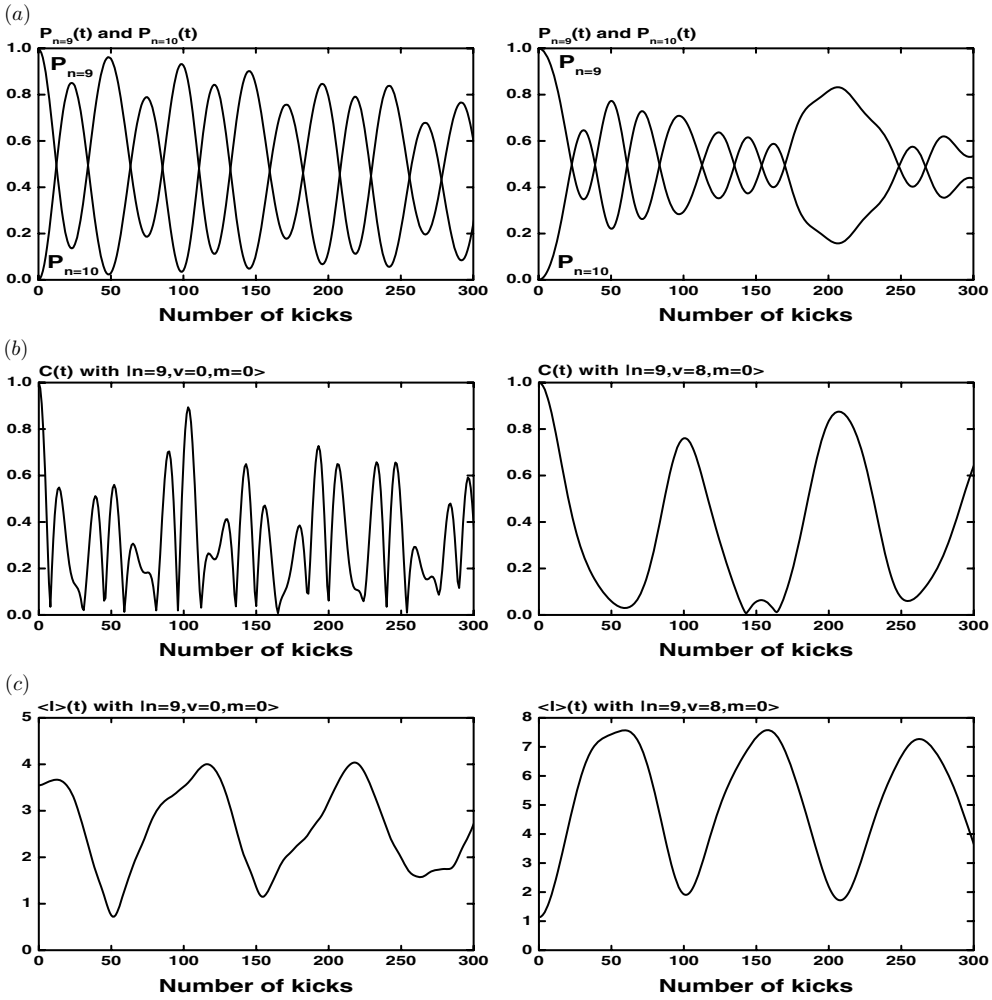

Figure 7. The dynamics of physical quantities of a kicked hydrogen atom in the uniform magnetic field. Comments are given in the text.

$H_0(\mathbf{r})$. Hence, we obtain an upper estimate for the time step $\tau < 4M\mu n^2$ (or $\tilde{\tau} < 4M\mu$) at $M = 3$ and $\mu \approx 0.28$ in accordance with (16).

For the initial parabolic state $|n_1 = 4, n_2 = 4, m = 0\rangle$ at the moment time $t = sT_+$ (or $\tilde{t} = s\tilde{T}_+$) figure 6 shows the calculated probabilities $P_{n=9}(t)$, $P_{n=10}(t)$ (a) and the autocorrelation function $C(t)$ (b) versus the number of kicks. For the initial spherical state $|n = 9, l = 0, m = 0\rangle$ at the moment time $t = sT_+$ (or $\tilde{t} = s\tilde{T}_+$) the same figure 6 displays the autocorrelation function $C(t)$ (c) and the expectation value of the angular momentum $\langle l\rangle(t)$ (d). These results markedly agree with those of [4, 5]. However, as noted in [4], the observed picture is more complicated than a two-state resonance with damping due to ionization and Rabi-like oscillations. Recall that the value of magnetic quantum number ($m = 0$) is conserved. The probability function $P_n(t)$, the autocorrelation function $C(t)$ and

the expectation value of the angular momentum $\langle l\rangle(t)$ are given by the expressions

$$P_n(t) = \sum_{l=1}^{n} \left| \int_0^{r_{\max}} \chi_l(r,t) R_{nl-1}(r) r^2 \, \mathrm{d}r \right|^2,$$
$$C(t) = \left| \sum_{l=1}^{N} \int_0^{r_{\max}} \overline{\chi}_l(r,t) \chi_l(r,0) r^2 \, \mathrm{d}r \right|, \tag{83}$$
$$\langle l\rangle(t) = \left| \sum_{l=1}^{N} (l-1) \int_0^{r_{\max}} \overline{\chi}_l(r,t) \chi_l(r,t) r^2 \, \mathrm{d}r \right|,$$

where $R_{nl}(r)$ is the normalized radial spherical discrete spectrum function of a free hydrogen atom.

Let us proceed to the situation when the hydrogen atom is kicked in the presence of a magnetic field parallel to the z-axis. In what follows we consider the magnetic field strength $\gamma = 1.472 \times 10^{-5}$ which is typical for the magnetic traps [8, 9]. Note that such a field strength is also of interest for the studies of recombination processes involving the excited states with $n = 8, 9, \ldots, 19$ and the metastable state with $n = 2$ of an antihydrogen atom, where the Lamb shift can be observed and thus the CPT invariance can be tested [54]. Table 2 shows the eigenenergies of the Zeeman states, calculated by the combined codes KANTBP [20] and POTHMF [30] of the multiplet $|n = 9, v = 0, \ldots, n-1, m = 0\rangle$.

We inspected the possibility of realizing the two-state resonance regime for the Zeeman states. Figure 7 shows the numerical results for the probabilities $P_{n=9}(t)$, $P_{n=10}(t)$ (a), the autocorrelation function $C(t)$ (b) and the expectation value of the angular momentum $\langle l\rangle(t)$ (c) at the moment time $t = sT$ for the initial Zeeman vibrational state $|n = 9, v = 0, m = 0\rangle$ (left) and rotational state $|n = 9, v = 8, m = 0\rangle$ (right) that, according to table 2, have the minimal and maximal energies within the $n = 9$ manifold. In contrast to the results presented in figure 6, a marked signature of two-state resonance regime is observed. A slight decay of the total probability $P_{n=9}(t) + P_{n=10}(t)$ is also observed. The role of initial Zeeman state in the realization of two-state resonance regime can be seen from figure 7: the picture obtained for the initial state $|n = 9, v = 8, m = 0\rangle$ is more complicated than the two-state resonance picture obtained for $|n = 9, v = 0, m = 0\rangle$.

6. Conclusions

We have presented a new computational approach to solve the TDSE, in which the partial (unitary) splitting of evolution operator and the FEM are efficiently combined. Particularly, to realize our approach in an explicit form, we have derived the second-, fourth-, and sixth-order approximations with respect to time step. Several numerical results have also been given which turn out to agree with the theoretical ones to a good extent.

Our approach would be worth being applied to the quantum control problem, some pre-experimental calculations in the atomic dynamics in traps and/or external-pulse fields, and other quantum calculations [7]. Further applications of the method may be associated with calculations of laser-induced recombination of antihydrogen in magnetic traps [10, 11], channeling of light nuclei in thin doped films [43] and potential scattering with confinement potentials [55]. In particular, the elaborated approach opens the possibility to take into account the influence of anharmonic perturbations on the dynamics of a wave packet in a driven two-dimensional oscillator, and to study the role of the anharmonic perturbations in the problem of transport in a two-dimensional quantum system under the influence of an external magnetic field and dissipative interaction with the environment [56].

Acknowledgments

The authors thank Professors Yu N Demkov, V P Gerdt, A M Ermolaev, V S Melezhik, V V Pupyshev and Y Uwano for useful discussions. This work was partly supported by grant I-1402/2004-2007 of the Bulgarian Foundation for Scientific Investigations, the grants RFBR 08-01-00604-a and 07-01-00660, the theme 09-6-1060-2005/2010 'Mathematical support of experimental and theoretical studies conducted by JINR', and the Scientific Center for Applied Research JINR.

Appendix. Taylor series of the logarithm evolution operator

Let us consider equation (2) with $U(t,s) \equiv U(t,s,\lambda=1)$

$$\frac{\partial U(t,s)}{\partial t} = -\mathrm{i}H(t)U(t,s), \tag{A.1}$$

where $s = t_c - \tau/2, t = t_c + \tau/2$. Denote $U(s,t) = U^{-1}(t,s)$. Using the operator identity

$$\frac{\partial U(s,t)}{\partial t} = -U(s,t)\frac{\partial U(t,s)}{\partial t}U(s,t), \tag{A.2}$$

the following relation for the operator $U(s,t)$ is valid:

$$\frac{\partial U(s,t)}{\partial t} = \mathrm{i}U(s,t)H(t). \tag{A.3}$$

Changing $t \longleftrightarrow s$ in equation (A.3), we find the operator equation for $U(t,s)$ with respect to the variable s

$$\frac{\partial U(t,s)}{\partial s} = \mathrm{i}U(t,s)H(s). \tag{A.4}$$

From here using equations (A.1), (A.4) and

$$2\frac{\partial U(t,s)}{\partial \tau} = \frac{\partial U(t,s)}{\partial t} - \frac{\partial U(t,s)}{\partial s}, \tag{A.5}$$

we obtain the derivative of the operator $U(t,s)$ with respect to the parameter τ at fixed t_c

$$2\frac{\partial U(t,s)}{\partial \tau} = -\mathrm{i}H(t)U(t,s) - \mathrm{i}U(t,s)H(s). \tag{A.6}$$

Using the well-known formula for the derivative of the exponential operator $U(t,s) = \exp(F)$, $F = -\mathrm{i}\tau A_k^{(M)}(t)$

$$\frac{\partial U(t,s)}{\partial \tau} = \int_0^1 \mathrm{d}x \exp(xF)\frac{\partial F}{\partial \tau}\exp(-xF)U(t,s), \tag{A.7}$$

and equation (19), we rewrite equation (A.6) in the following form:

$$2\sum_{j=0}\frac{1}{(j+1)!}(adF)^j\,\dot{F} = -\mathrm{i}H(t) - \mathrm{i}\sum_{j=0}\frac{1}{j!}(adF)^j\,H(s). \tag{A.8}$$

In the explicit form with equations (10) and (12) taken into account

$$-\sum_{q=0}\frac{(-\mathrm{i})^q\tau^q}{q!}\left(ad\sum_{m=0}\tau^m\check{A}_{(m)}(t_c)\right)^q\sum_{n=0}\tau^n Q_{qn}(t_c) = \sum_{i=0}\frac{\tau^i}{2^{i+1}i!}\partial_t^i H(t_c), \tag{A.9}$$

where

$$Q_{qn}(t_c) = \frac{(-1)^n}{2^{n+1}n!}\partial_t^n H(t_c) - \frac{n+1}{q+1}\check{A}_{(n)}(t_c). \tag{A.10}$$

Then the unknown coefficients $\check{A}_{(j)}(t_c)$ are calculated explicitly from a set of recurrence equations

$$(j+1)\check{A}_{(j)}(t_c) = \frac{1+(-1)^j}{2^{j+1}\,j!}\partial_t^j H(t_c) + \sum_{q=1}^{j}\sum_{n=0}^{j-q}\sum_{l_1,\ldots,l_q=0}^{n+q+\sum_{i=1}^{q} l_i = j} \frac{(-\mathrm{i})^q\, B^n_{l_1,\ldots,l_q}(t_c)}{q!}, \tag{A.11}$$

$$B^n_{l_1,\ldots,l_q}(t_c) = (ad\check{A}_{(l_1)}(t_c))\ldots(ad\check{A}_{(l_q)}(t_c))Q_{qn}(t_c).$$

References

[1] Derbov V L, Melnikov L A, Umansky I M and Vinitsky S I 1997 *Phys. Rev.* A **55** 3394–400
[2] Gusev A, Gerdt V, Kaschiev M, Rostovtsev V, Samoylov V, Tupikova T, Uwano Yo and Vinitsky S 2005 *Lecture Notes Comput. Sci.* **3718** 244–58
[3] Gusev A, Gerdt V, Kaschiev M, Rostovtsev V, Samoylov V, Tupikova T, Uwano Y and Vinitsky S 2007 *PEPAN Lett.* **4** 253–9
[4] Dhar A K, Nagarajan M A, Israilev F M and Whitehead R R 1983 *J. Phys. B: At. Mol. Phys.* **16** L17–22
[5] Klews M and Schweizer W 2001 *Phys. Rev.* A **64** 053403–1–5
[6] Popov Yu V, Kouzakov K A, Vinitsky S I and Gusev A A 2007 *Phys. Atom . Nucl .* **70** 601–6
[7] Butkovskiy A G and Samoilenko Yu I 1990 *Control of Quantum-Mechanical Processes and Systems* (Dordrecht Hardbound: Kluwer)
[8] Holzscheiter M H and Charlton M 1999 *Rep. Prog. Phys.* **62** 1–60
[9] Amoretti M *et al* 2004 *Phys. Lett.* B **590** 133–42
[10] Serov V V, Derbov V L and Vinitsky S I 2007 *Opt. spectrosc.* **102** 557–61
[11] Chuluunbaatar O, Gusev A A, Derbov V L, Kaschiev M S, Serov V V, Melnikov L A and Vinitsky S I 2007 *J. Phys. A: Math. Theor.* **40** 11485–524
[12] Wetzels A, Gurtler A, Noordam L D and Robicheaux F 2006 *Phys. Rev.* A **73** 062507–1–8
[13] Misicu S, Rizea M and Greiner W 2001 *J. Phys. G: Nucl. Part. Phys.* **27** 993–1003
[14] Serov V V, Derbov V L, Joulakian B B and Vinitsky S I 2007 *Phys. Rev.* A **75** 012715–1–9
[15] Chuluunbaatar O, Joulakian B B, Puzynin I V, Tsookhuu Kh and Vinitsky S I 2008 *J. Phys. B: At. Mol. Opt. Phys.* **41** 015204–1–6
[16] Ermolaev A M, Puzynin I V, Selin A V and Vinitsky S I 1999 *Phys. Rev.* A **60** 4831–45
[17] Ermolaev A M and Selin A V 2000 *Phys. Rev.* A **62** 015401–1–4
[18] Melezhik V S, Kim J I and Schmelcher P 2007 *Phys. Rev.* A **76** 053611–1–15
[19] Puzynin I V, Boyadjiev T L, Vinitsky S I, Zemlyanaya E V, Puzynina T P and Chuluunbaatar O 2007 *PEPAN* **38** 144–232
[20] Chuluunbaatar O, Gusev A A, Abrashkevich A G, Amaya-Tapia A, Kaschiev M S, Larsen S Y and Vinitsky S I 2007 *Comput. Phys. Commun.* **177** 649–75
[21] Pupyshev V V 2004 *PEPAN* **35** 256–347
[22] Magnus W 1954 *Commun. Pure Appl. Math.* **7** 649–73
[23] Puzynin I V, Selin A V and Vinitsky S I 1999 *Comput. Phys. Commun.* **123** 1–6
[24] Puzynin I V, Selin A V and Vinitsky S I 2000 *Comput. Phys. Commun.* **126** 158–61
[25] Selin A V 2002 *Comput. Math. Math. Phys.* **42** 901–14
[26] Strang G and Fix G 1973 *An Analisys of The Finite Element Method* (Englewood Cliffs, NJ: Prentice-Hall)
[27] Bathe K J 1982 *Finite Element Procedures in Engineering Analysis* (Englewood Cliffs, NJ: Prentice-Hall)
[28] Abrashkevich A G, Abrashkevich D G, Kaschiev M S and Puzynin I V 1995 *Comput. Phys. Commun.* **85** 40–65
[29] Abrashkevich A G, Kaschiev M S and Vinitsky S I 2000 *J. Comp. Phys.* **163** 328–48
[30] Chuluunbaatar O, Gusev A A, Gerdt V P, Rostovtsev V A, Vinitsky S I, Abrashkevich A G, Kaschiev M S and Serov V V 2008 *Comput. Phys. Commun.* **178** 301–30
[31] Wilcox R M 1967 *J. Math. Phys.* **8** 962–82
[32] Klarsfeld S and Oteo J A 1989 *Phys. Rev.* A **39** 3270–73
[33] Pechukas P and Light J C 1966 *J. Chem. Phys.* **44** 3897–912
[34] Dattoli G, Gallardo J and Torre A 1986 *J. Math. Phys.* **27** 772–80
[35] Saff E B and Varga R S 1975 *Numer. Math.* **25** 1–14
[36] Saff E B and Varga R S 1977 *Padé and Rational Approximation, Theory and Applications* (New York: Academic) pp 195–213
[37] Saff E B and Varga R S 1978 *Numer. Math.* **30** 241–66
[38] Samarskii A A 1977 *Theory of Difference Schemes* (Moscow: Nauka) (in Russian)

[39] Crank J and Nicolson P 1947 *Proc. Cambridge Philos. Soc.* **43** 50–67
[40] Hochbruck M and Lubich Ch 2003 *SIAM J. Numer. Anal.* **41** 945–63
[41] Kantorovich L V and Krylov V I 1964 *Approximate Methods of Higher Analysis* (New York: Wiley)
[42] Melnikov L A, Derbov V L and Bychenkov A I 1999 *Phys. Rev.* E **60** 7490–6
[43] Demkov Yu N and Meyer J D 2004 *Eur. Phys. J.* B **42** 361–5
[44] Wiedemann H, Mostowski J and Haake F 1994 *Phys. Rev.* A **49** 1171–6
[45] Reinhold C O, Yoshida S, Burgdörfer J, Tannian B E, Stokely C L and Dunning F B 2001 *J. Phys. B: At. Mol. Opt. Phys.* **34** L551–8
[46] Persson E, Yoshida S, Tong X-M, Reinhold C O and Burgdörfer J 2003 *Phys. Rev.* A **68** 063406–1–15
[47] Reinhold C O, Zhao W, Lancaster J C, Dunning F B, Persson E, Arbó D G, Yoshida S and Burgdörfer J 2004 *Phys. Rev.* A **70** 033402–1–7
[48] Zhao W, Mestayer J J, Lancaster J C, Dunning F B, Reinhold C O, Yoshida S and Burgdörfer J 2005 *Phys. Rev. Lett.* **95** 163007–1–4
[49] Reinhold C O, Yoshida S, Burgdörfer J, Zhao W, Mestayer J J, Lancaster J C and Dunning F B 2006 *Phys. Rev.* A **73** 033420–1–6
[50] Melezhik V S 1995 *Phys. Rev.* A **52** R3393–6
[51] Tarter C B 1970 *J. Math. Phys.* **11** 3192–5
[52] Engenfield M J 1972 *Group Theory and the Coulomb Problem* (Victoria: Monash university)
[53] Matos-Abiague A and Kouzakov K A 2003 *Phys. Rev.* A **68** 017401–1–3
[54] Udem Th, Huber A, Gross B, Reichert J, Prevedelli M, Weitz M and Hänsch T W 1997 *Phys. Rev. Lett.* **79** 2646–9
[55] Kim J I, Melezhik V S and Schmelcher P 2006 *Phys. Rev. Lett.* **97** 193203–1–4
[56] Kalandarov Sh A, Kanokov Z, Adamian G G and Antonenko N V 2007 *Phys. Rev.* E **75** 031115–1–16